International Atomic Energy Agency

INDC(POL)-014
Distr. NG

INDC INTERNATIONAL NUCLEAR DATA COMMITTEE

Compilation and evaluation of high energy γ-ray standards from nuclear reactions

A. Marcinkowski and B. Mariański

The Andrzej Sołtan Institute for Nuclear Studies
Hoża 69, 00-681 Warszawa, Poland

Work performed under the Coordinated Research Project "Update of X-and γ-ray Decay Data Standards for Detector Calibration"

February 1999

IAEA NUCLEAR DATA SECTION, WAGRAMERSTRASSE 5, A-1400 VIENNA

Reproduced by the IAEA in Austria
February 1999

INDC(POL)-014
Distr. NG

Compilation and evaluation of high energy γ-ray standards from nuclear reactions

A. Marcinkowski and B. Mariański

The Andrzej Sołtan Institute for Nuclear Studies
Hoża 69, 00-681 Warszawa, Poland

Work performed under the Coordinated Research Project
"Update of X-and γ-ray Decay Data Standards for Detector Calibration"

Date of Manuscript: November 1998

Report INR(Z-P1)-No 01/1998

February 1999

Compilation and evaluation of high energy γ-ray standards from nuclear reactions.

Part 1: Evaluation of emission probabilities of γ-rays with energies 4.44 MeV and 15.11 MeV from $^{12}C^*$, preparation of the list of reactions suitable for production of the above mentioned excited radionuclide and compilation and evaluation of cross sections for these reactions including inelastic proton scattering on ^{12}C and radiative capture on ^{11}B.

by A. Marcinkowski and B. Marianski

The strongest deexcitation line in $^{12}C^*$, at 4.438 MeV results from the decay of its first excited state at 4.439 MeV. Excited states above the 4.439 MeV level decay primarily by breakup into α-particles, and hence they are not important sources of γ-ray lines [Led78,Fir96].

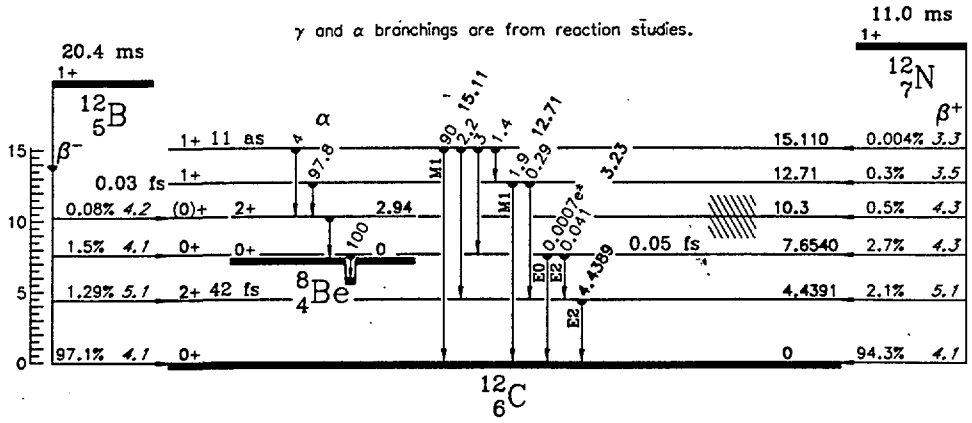

An exception is the 15.11 MeV level, which, because of conservation of isotopic spin, cannot decay by emitting α-particles and hence deexcites only by γ-ray emission. The cross sections for exciting this level were compiled in ref. [Ram79], where it was found that the intensity of the 15.1 MeV line is at most about 2% of the 4.438 MeV line intensity. At proton energies lower than 23 MeV the overall contribution of the higher excitet states to the 4.44 MeV γ-rays is less than 0.5 mb.

The various excitation modes of the 4.439 MeV and the 15.11 MeV levels involving proton and α-particle projectiles are following:

$^{11}B(p,\gamma)^{12}C^*$,
$^{12}C(p,p')^{12}C^*$,
$^{12}C(\alpha,\alpha')^{12}C^*$,
$^{14}N(p,2p)^{12}C^*$,
$^{14}N(\alpha,\alpha p)^{12}C^*$,
$^{16}O(p,\alpha p)^{12}C^*$,
$^{16}O(\alpha,2\alpha)^{12}C^*$,

the reactions,

$^{12}C(p,2p)^{11}B^*$,
$^{12}C(\alpha,\alpha p)^{11}B^*$,

excite the 4.444 MeV level in ^{11}B, which has an energy threshold of 22 MeV. The resulting γ-line of energy 4.443 MeV cannot be resolved from the 4.439 MeV one because the kinematical Doppler broadning blends the two into a single feature.

1. The $^{11}B(p,\gamma)^{12}C^*$ reaction

Proton capture by ^{11}B at incident resonance energy 163 keV [But59] populates the level at excitation energy of 16.1058 MeV in ^{12}C, which decays to the first excitet level at 4.439 MeV producing the cascading γ-rays of energies 4.44 MeV and 11.7 MeV with intensity of 92 kwanta per 100 decays [Zob68]. The other resonances in the proton capture yield curve are of less practical importance. We list these data taken from Butler [But59],

proton energy	γ-ray energies	cross section	width	reference
163 keV	16.11, 11.68, 4.43	0.157 mb	7 keV	[Cr56, Hu53],
675 keV	12.15, 4.43	0.050 mb	322 keV	[Hu53],
1388 keV	17.23, 12.80	0.053 mb	1270 keV	[Hu53, De57],
2630 keV	13.94, 4.43, 2.14		300 keV	[Ba55, Ho55].

However, in applications of the proton capture reaction as a source of standard γ-rays common use is made of the primary high-energy γ-transitions from the capturing states (within the energy spread of the proton projectiles) to the ground state and the subsequent excited states of ^{12}C.

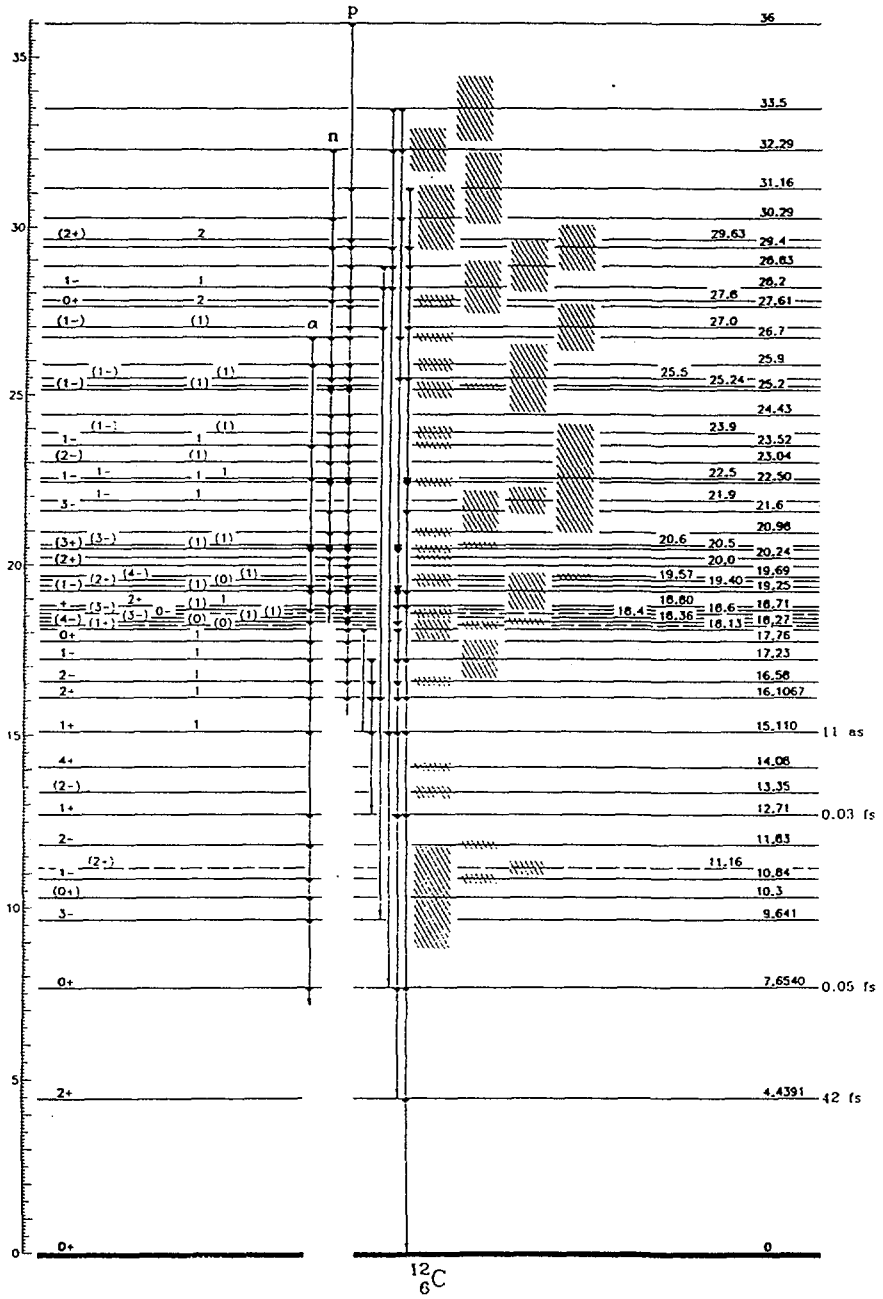

The variable energies of these γ-rays depend on the incident laboratory energy E_p, the binding energy of a proton in ^{12}C, B_p=15.96 MeV, and of the energy of the excited level E_x,

$$E_{\gamma x} = E_p(\frac{11}{12})^2 + B_p - E_x \quad . \tag{1}$$

The width of the corresponding peaks in the measured γ-ray spectra depends on the target thickness which adds to the energy resolution of the proton beam usually as a dominant factor (tens of μg to tens of mg per cm^2 are used at the incident energies considered here). Below we show standard spectra of the primary γ-rays detected with use of large Na(J) crystal with anticoincidence shield [Sno77,Ang83].

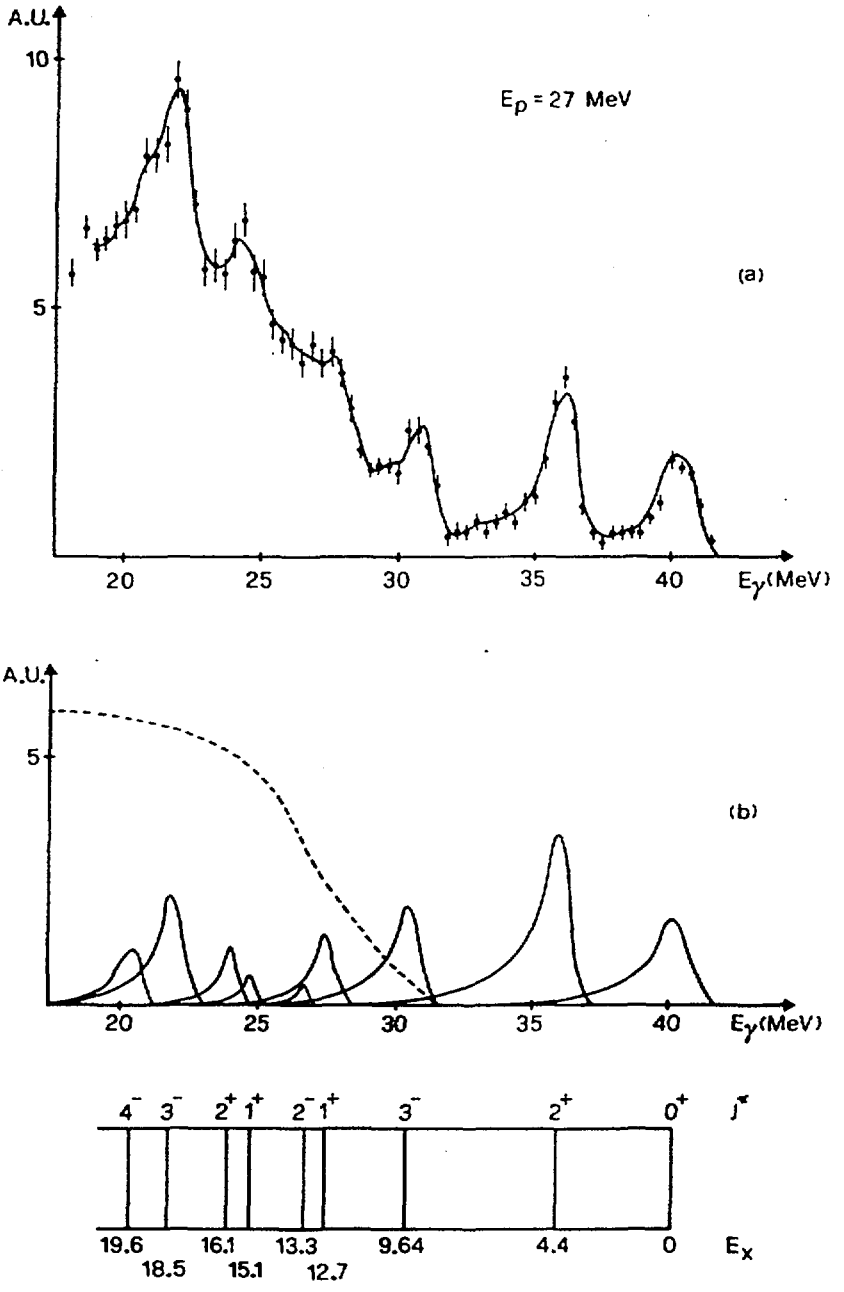

, The capture photon spectrum; the full line is the fit. (b) Unfolded response functions for the ınsitions to the reported ^{12}C levels; the dotted line gives the background

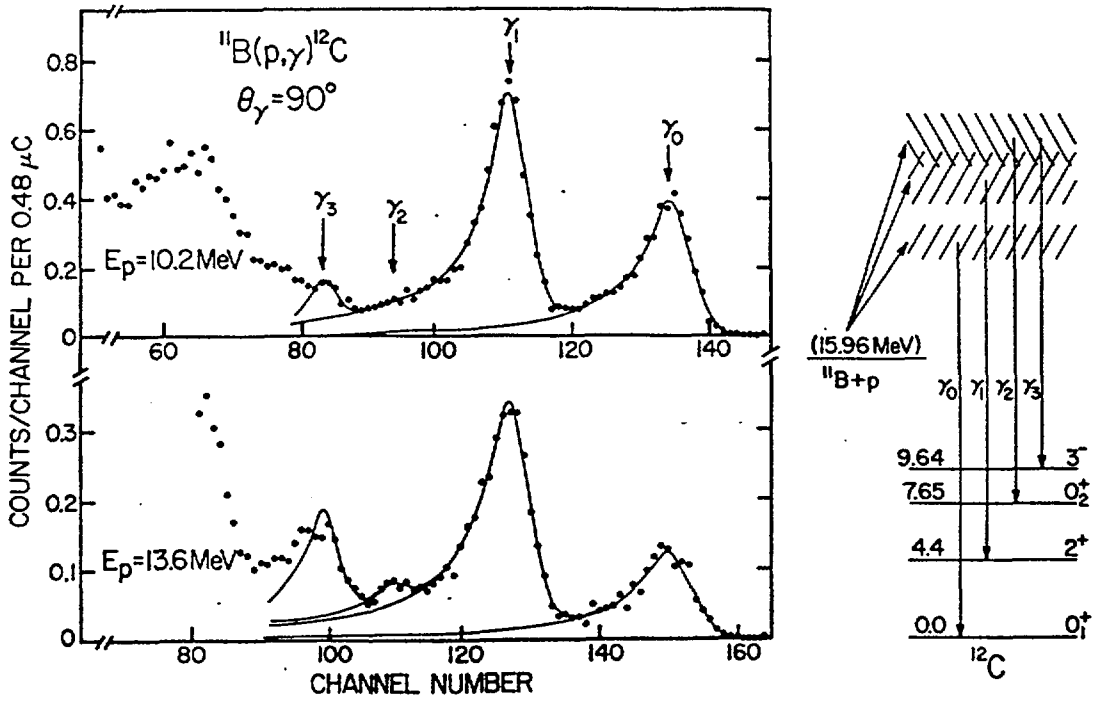

The left portion of the figure shows the high-energy portion of γ-ray spectra obtained in the proton bombardment of ^{11}B. The solid curves represent a least-squares fit to the data using a sum of four γ-ray lineshapes. The right portion of the figure indicates an energy-level diagram for the levels of interest.

Yield curves measured at 90° have been reported for γ_0 and γ_1 in about 20 keV steps up to 5.4 MeV [Bai55], for γ_0 in 75 keV steps between 4.0 anf 7.7 MeV [Gem59], for γ_0 in 100 keV steps between 2.6 and 11.4 MeV and for γ_1 in 200 keV steps between 6.0 and 11.4 MeV [Gov61] and for both γ_0 and γ_1 in 100 kev steps between 6.0 and 13.2 MeV [Bec63]. All these data are consistent in shape and magnitude and agree with those reported in [All64] label *A* in the comparison below where the curves are arbitrarily displaced vertically.

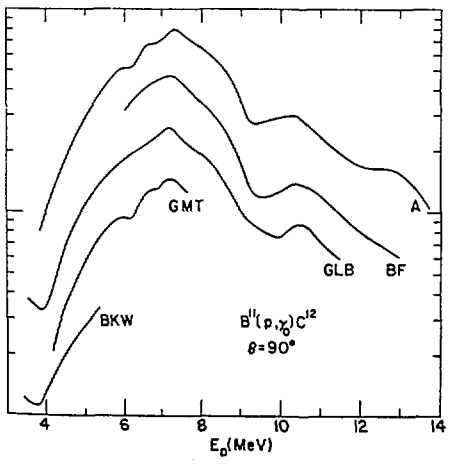

The 90° yield curve for γ_0 as variously reported.

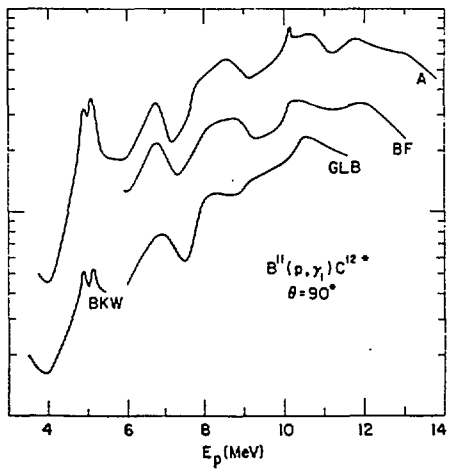

The 90° yield curve for γ_1 as variously reported.

Angular distributions were measured for γ_0 and γ_1 over the range from 3.89 to 13.83 MeV [All64]. The distributions for γ_0 vary but little and peak near 90° over the entire energy range. The anisotropy is large, the peak intensity being about twice the extrapolated yields at 0° and 189°. The curves are not symmetric about 90°, the yield being noticeably greater in the forward direction as was shown in [All64],

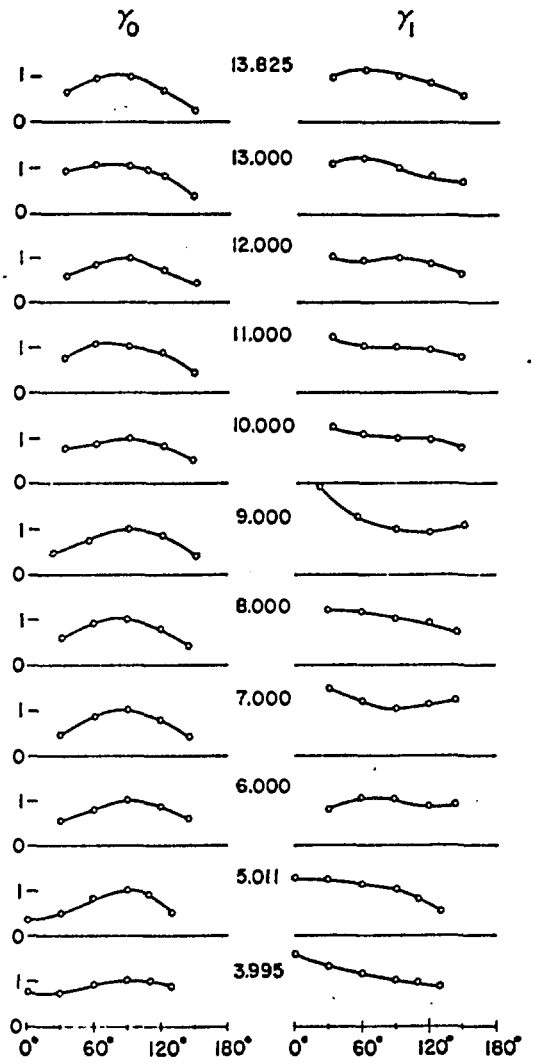

A sampling of angular distributions of γ_0 and of γ_1. Angular distributions were taken about every 50 keV.

As compared with the γ_0 distributions, the γ_1 curves in Fig. 4 vary more and usually are less anisotropic. The differential cross section can be expressed as,

$$\frac{d\sigma}{d\Omega} = A_0[1+\sum_{n>0} a_n P_n(\theta)] \quad , \tag{2}$$

so that the total cross section is $4\pi A_0$. If a strong quadrupole component is present in the primary capture radiation, terms up to and including P_4 might be required; for dipole radiation, terms up to and including P_2 would be sufficient. Presence of terms higher than P_4 would indicate the presence of radiation of multipolarity higher than quadrupole. Actually a_3 and a_4 were usually

found to be small. All the multipole expansion coefficient for proton energies up to 14 MeV obtained in [All64] are presented in a graphic form,

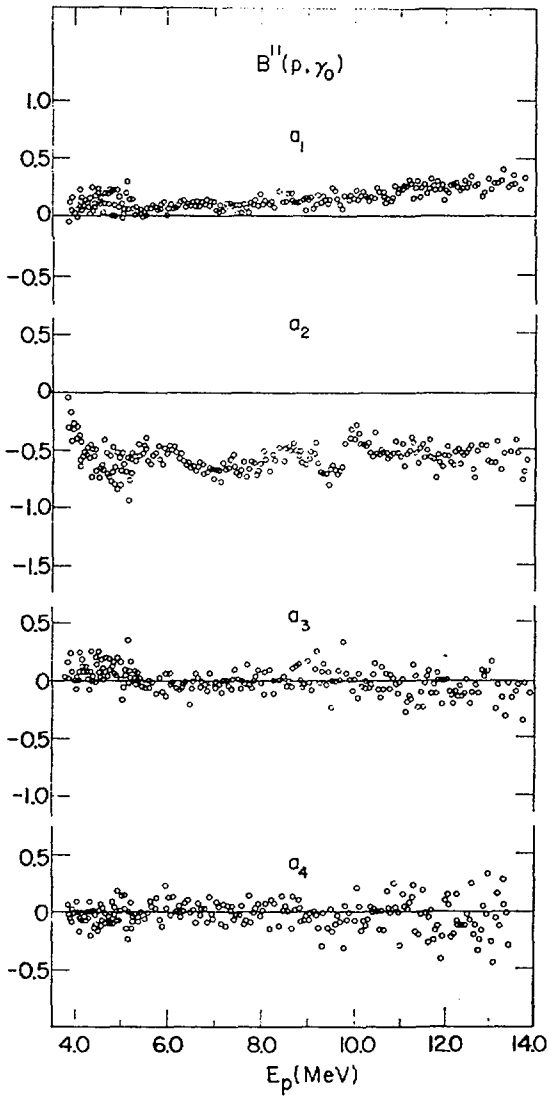

The coefficients a_n obtained by expanding the angular distributions of γ_0 into a series of Legendre polynomials $W(\theta) = A_0(1+\Sigma_n a_n P_n(\cos\theta))$. The finite solid angle subtended by the detector attenuates a_2 by about 3 %.

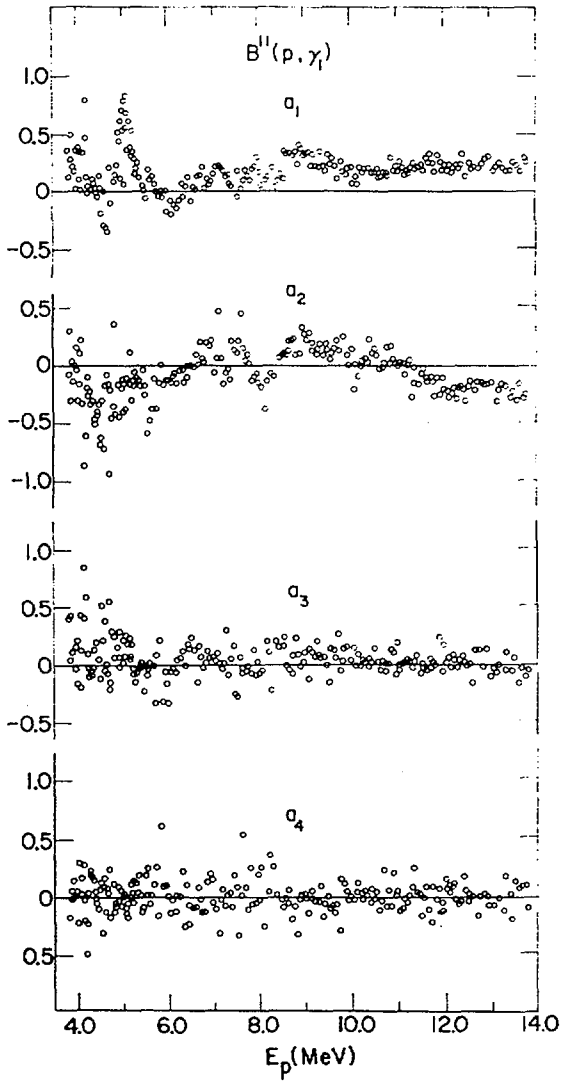

The coefficients a_n obtained by expanding the angular distributions of γ_1 into a series of Legendre polynomials $W(\theta) = A_0(1+\Sigma_n a_n P_n(\cos\theta))$.

The expansion coefficients for the γ_0-rays compiled from [Ker69,Bras72,Mat75,Ang83] cover the incident proton energy range reaching 90 MeV,

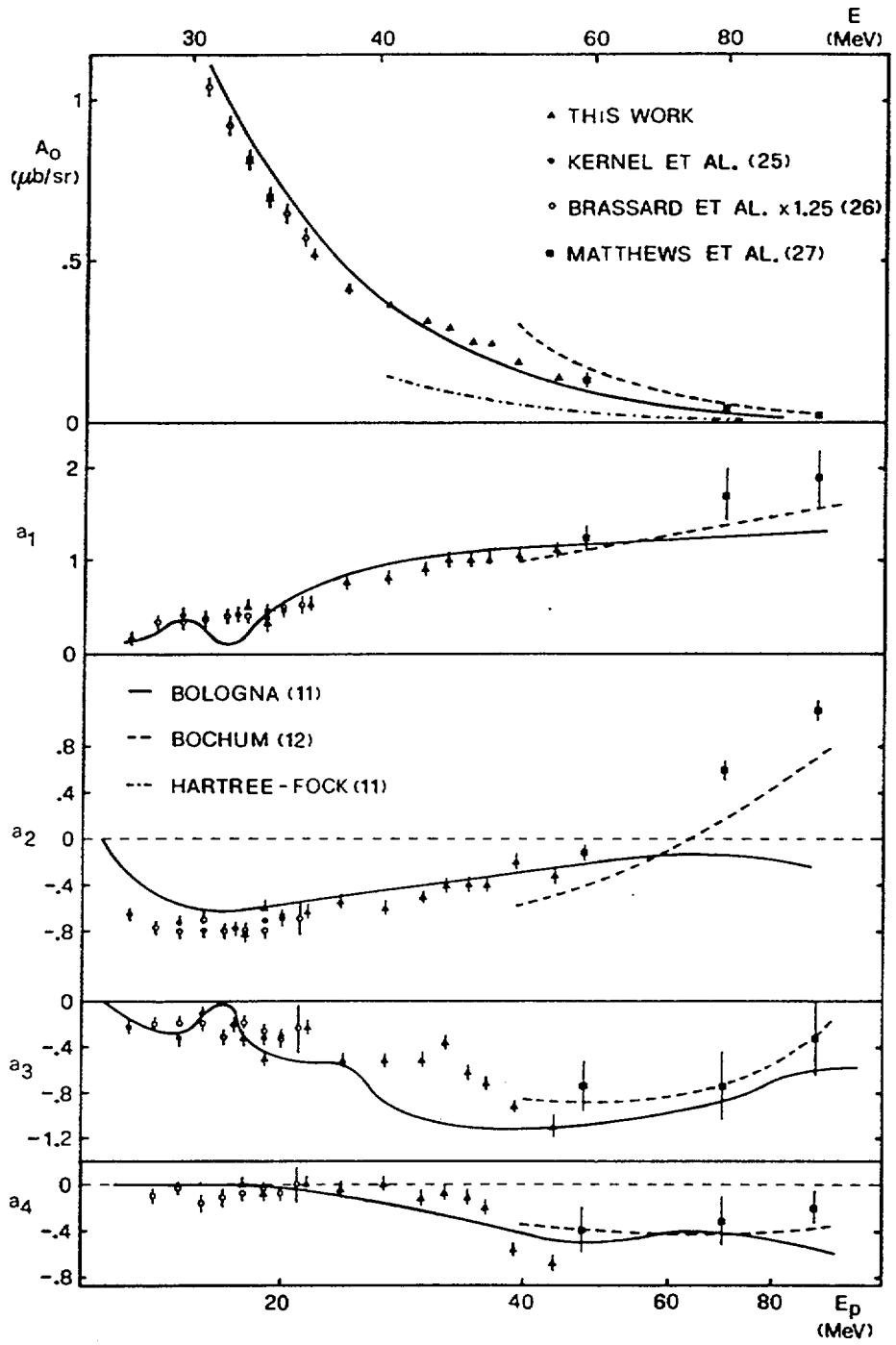

Multipole expansion coefficients for the (p, γ_0) cross section compared with the available theoretical calculations.

The expansion coefficient for the γ_1-, γ_3-, $\gamma_7+\gamma_8$-, $\gamma_{10}+\gamma_{11}$-, $\gamma_{18}-\gamma_{19}$-, $\gamma_{19}+\gamma_{24}+\gamma_{29}$-rays obtained in [Ang83] extend over the proton energies up to 43 MeV and are shown in the following three figures.

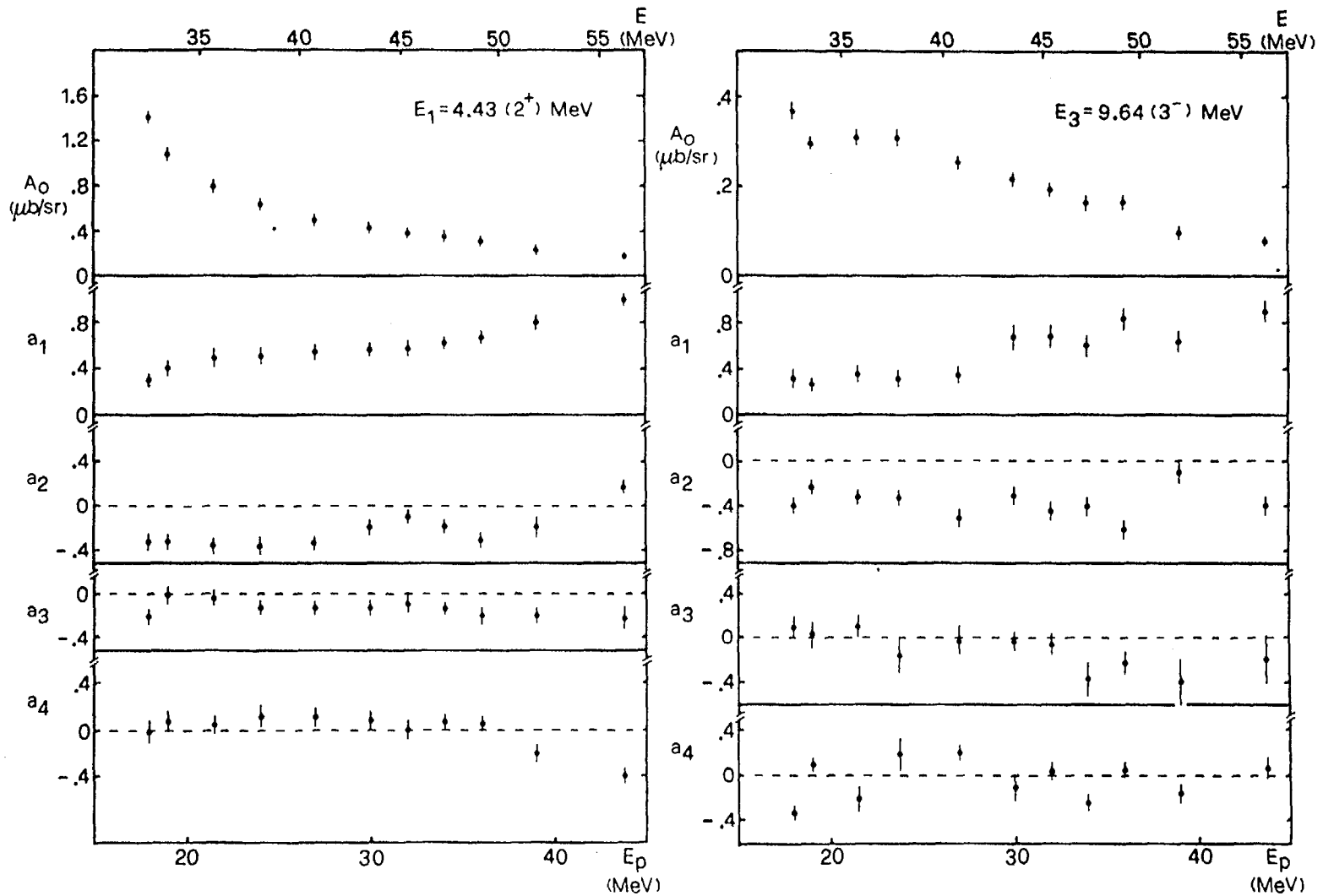

The multipole expansion (1) coefficients $A_0 = \sigma(E)/4\pi$ and a_L for the capture cross sections to the first and third excited states in ^{12}C.

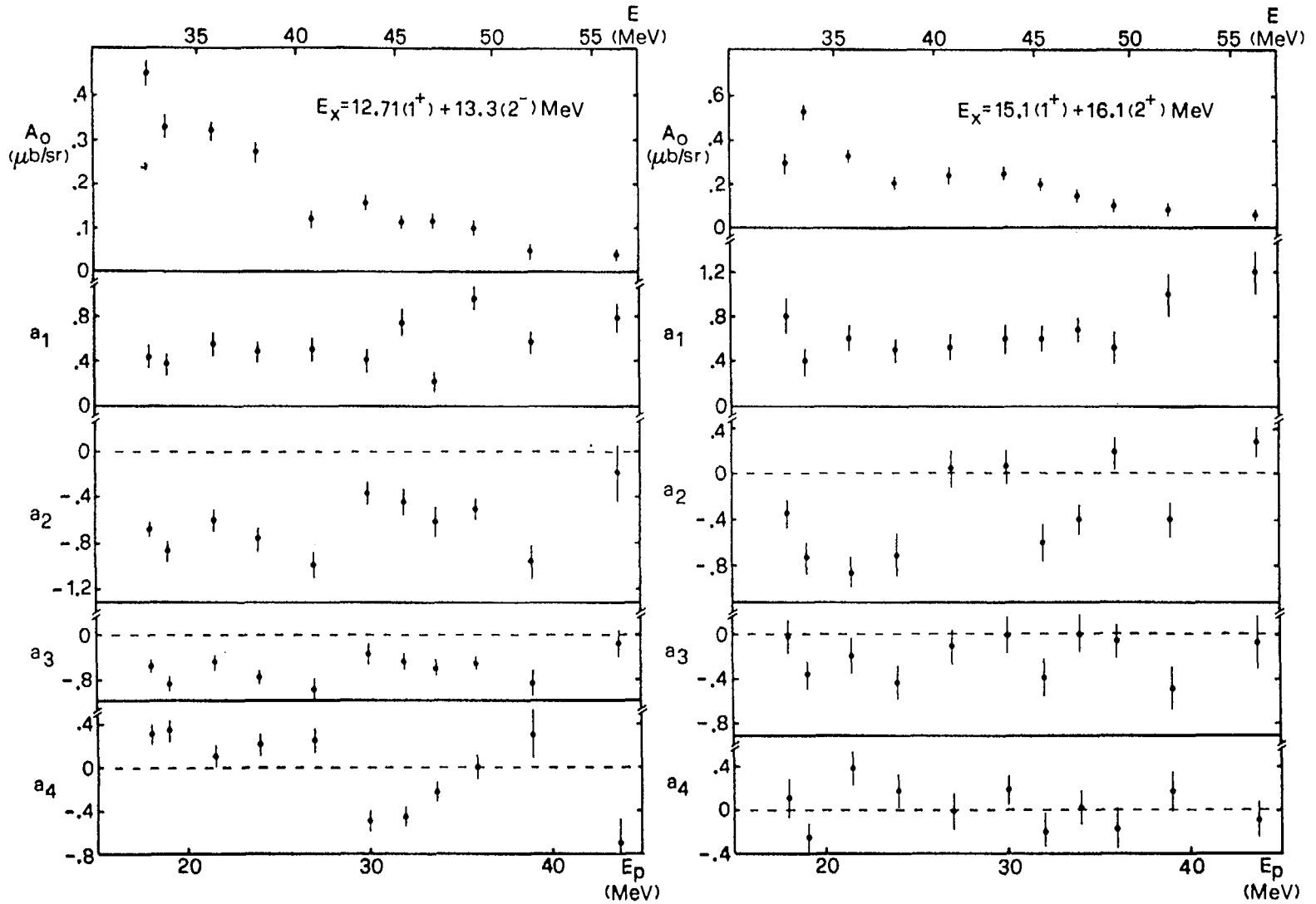

The multipole expansion (1) coefficient $A_0 = \sigma(E)/4\pi$ and a_L for the capture cross sections to the two groups of ^{12}C states around 13 MeV and 15 MeV.

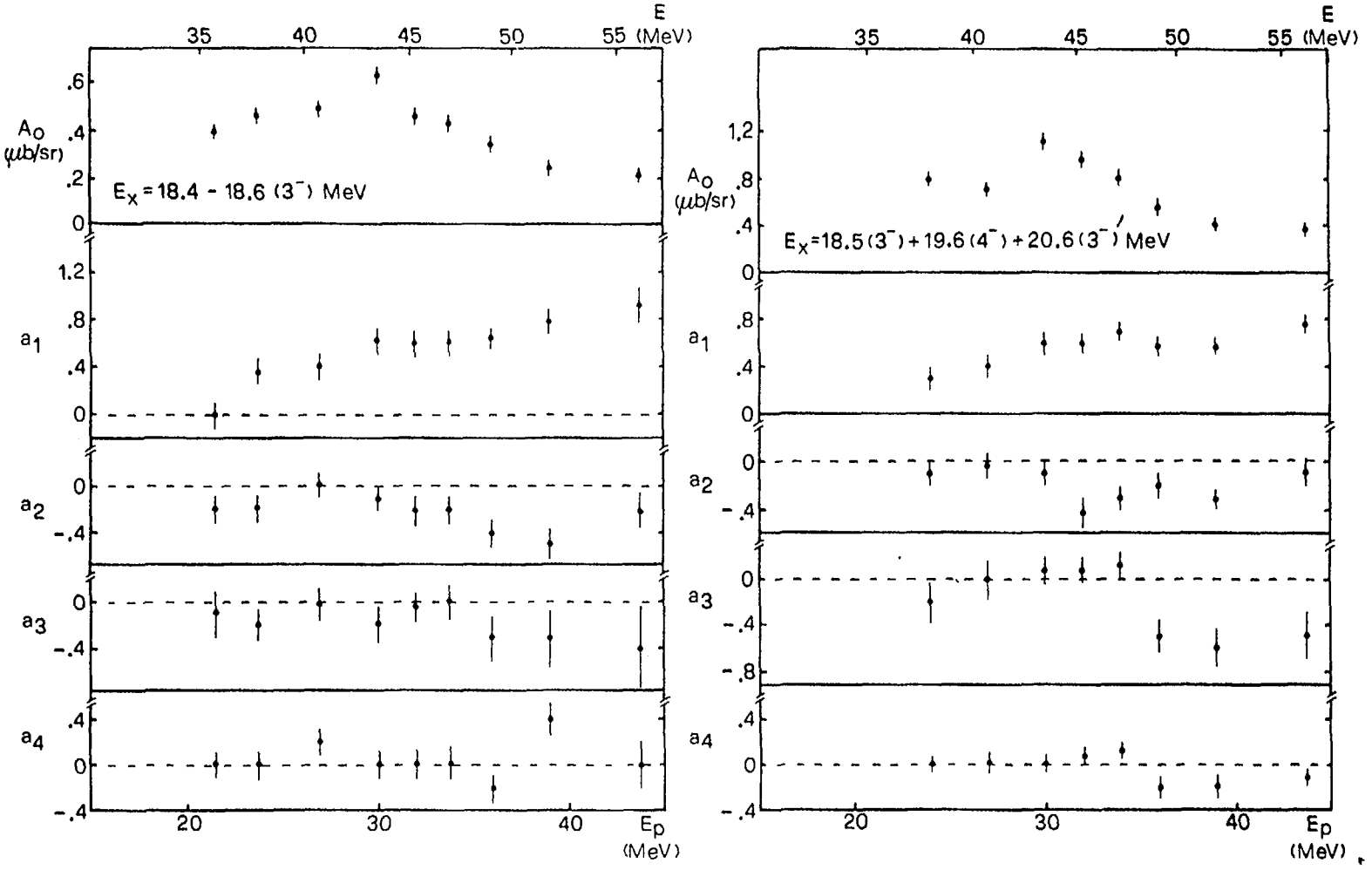

The multipole expansion (1) coefficients $A_0 = \sigma(E)/4\pi$ and a_L for the capture cross sections to the group of ^{12}C states around 19 MeV. The contribution of the 3^- doublet at 18.4–18.6 MeV is reported separately.

Differential cross sections for the γ_0-rays in numerical form are also available from [Ang83],

Experimental differential cross section $(d\sigma/d\Omega)_{lab}$ for the (p, γ_0) channel (μb/sr)

E_p	σ_L						
	34	45	60	75	90	105	120
18	0.76±0.037	1.01±0.051	1.26±0.056	1.20±0.063	1.17±0.063	0.885±0.045	0.58 ±0.030
19	0.65±0.034	0.90±0.027	1.03±0.051	1.08±0.060	0.85±0.050	0.65 ±0.037	0.48 ±0.027
21.5	0.59±0.026	0.76±0.042	0.79±0.038	0.74±0.040	0.75±0.041	0.49 ±0.028	0.33 ±0.019
24	0.51±0.029	0.66±0.019	0.64±0.032	0.63±0.037	0.59±0.033	0.32 ±0.018	0.20 ±0.012
27	0.47±0.026	0.58±0.031	0.65±0.030	0.58±0.031	0.48±0.027	0.29 ±0.017	0.15 ±0.010
30	0.52±0.024	0.52±0.028	0.57±0.026	0.47±0.025	0.40±0.022	0.25 ±0.011	0.128±0.008
32	0.47±0.021	0.48±0.025	0.52±0.021	0.47±0.025	0.32±0.018	0.24 ±0.014	0.10 ±0.006
34	0.41±0.021	0.42±0.021	0.46±0.021	0.42±0.002	0.29±0.016	0.15 ±0.009	0.078±0.005
36	0.39±0.017	0.46±0.023	0.47±0.021	0.38±0.018	0.30±0.016	0.13 ±0.008	0.07 ±0.005
39	0.33±0.016	0.40±0.020	0.42±0.019	0.27±0.014	0.19±0.011	0.06 ±0.004	0.05 ±0.004
43.7	0.19±0.010	0.37±0.018	0.33±0.014	0.21±0.011	0.16±0.009	0.04 ±0.004	0.026±0.002

The anle integrated cross sections for production of the primary γ_0- and γ_1-rays are presented as a function of proton energy up to 14 MeV in [All64],

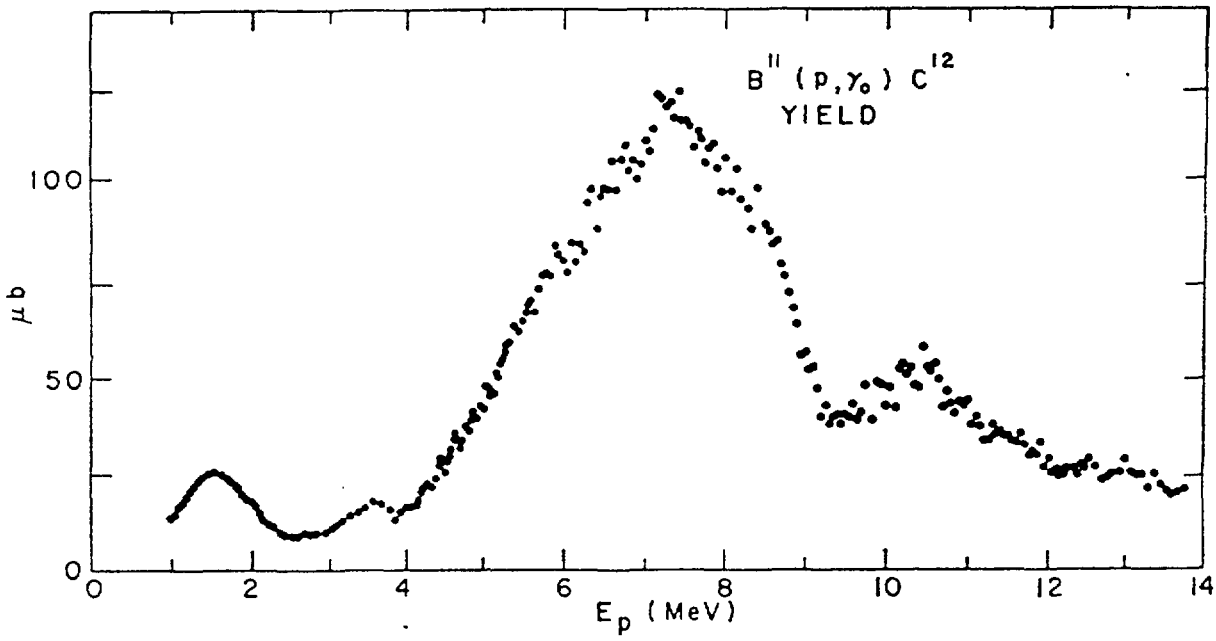

Total cross section for the $B^{11}(p, \gamma_0)C^{12}$ reaction as a function of energy.

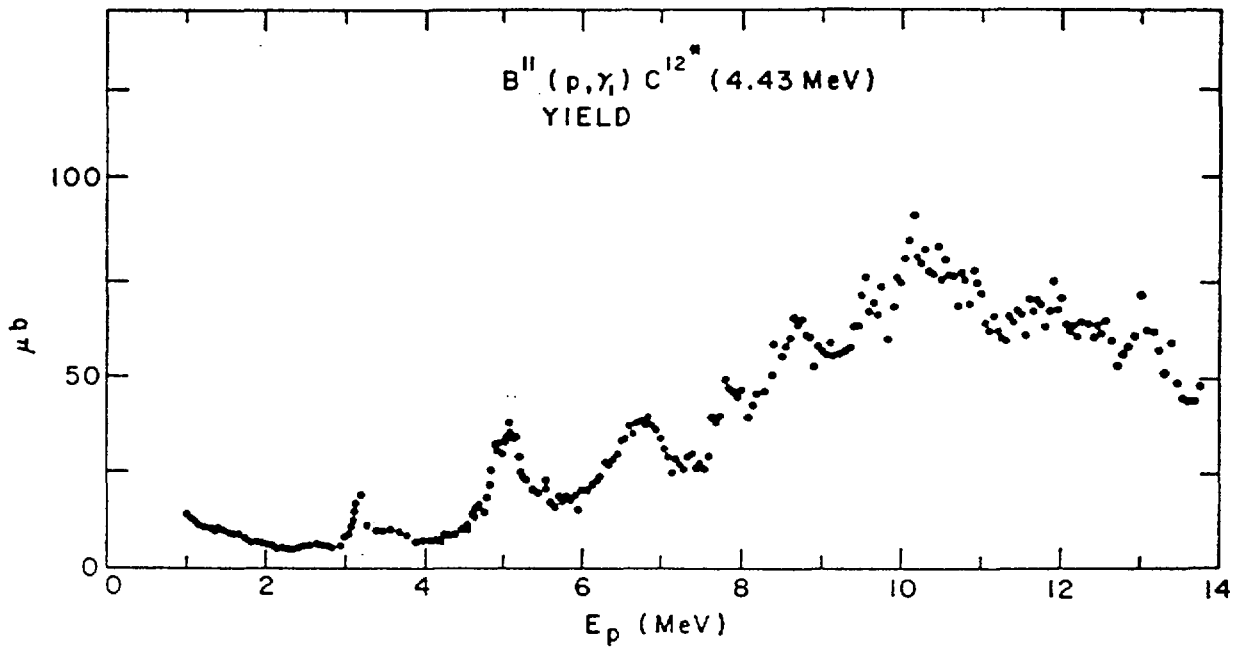

Total cross section for the $B^{11}(p, \gamma_1)C^{12}$ reaction as a function of energy.

and the total cross sections for the primary γ-rays to the higher excited states of ^{12}C were obtained in [Ang83],

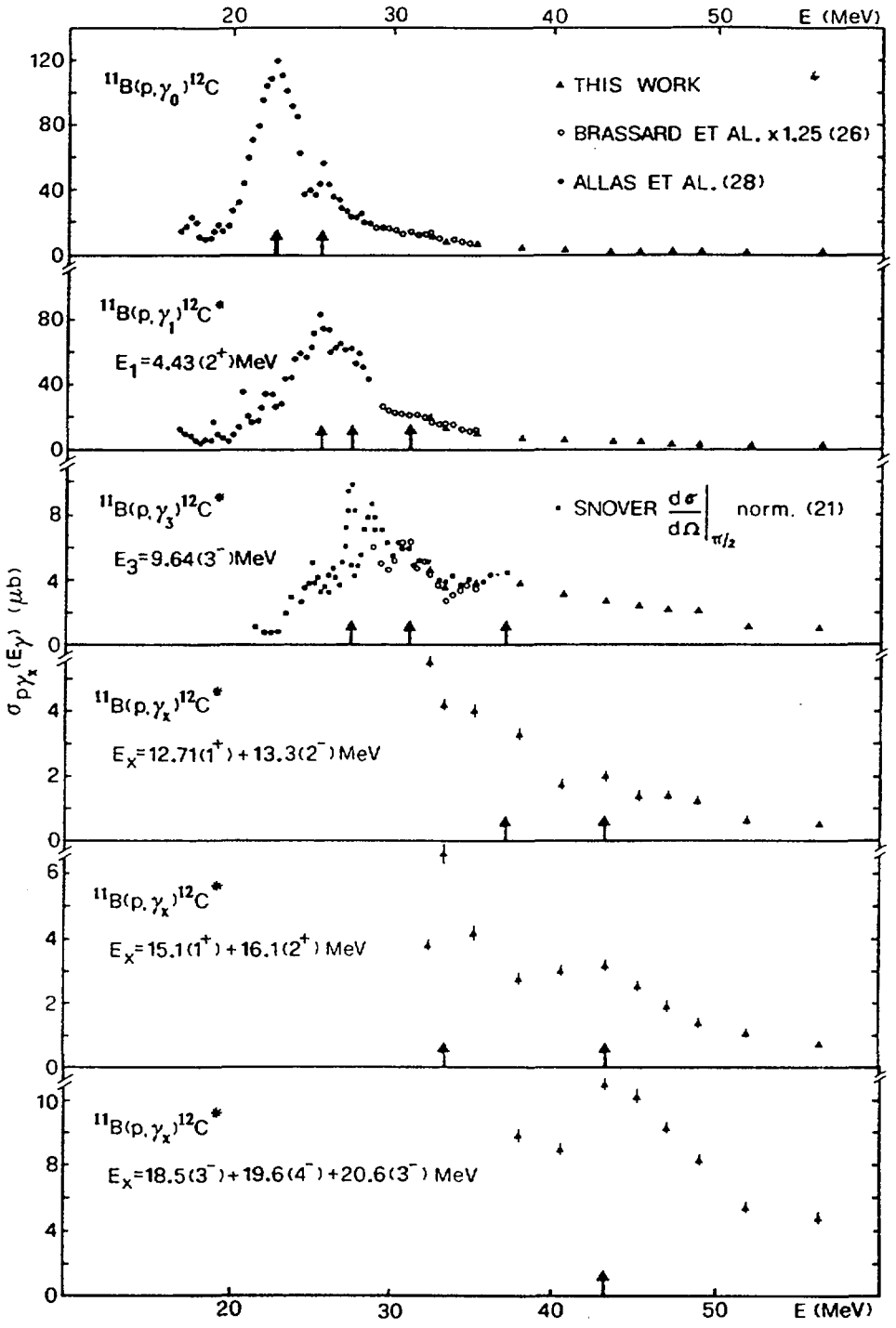

Capture cross sections to the various states of ^{12}C as a function of the excitation energy. The arrows show the position of the resonances.

Below are shown also the 90° cross sections for the production of the γ_0-, γ_1-, γ_2- and γ_3-rays reported in [Sno77],

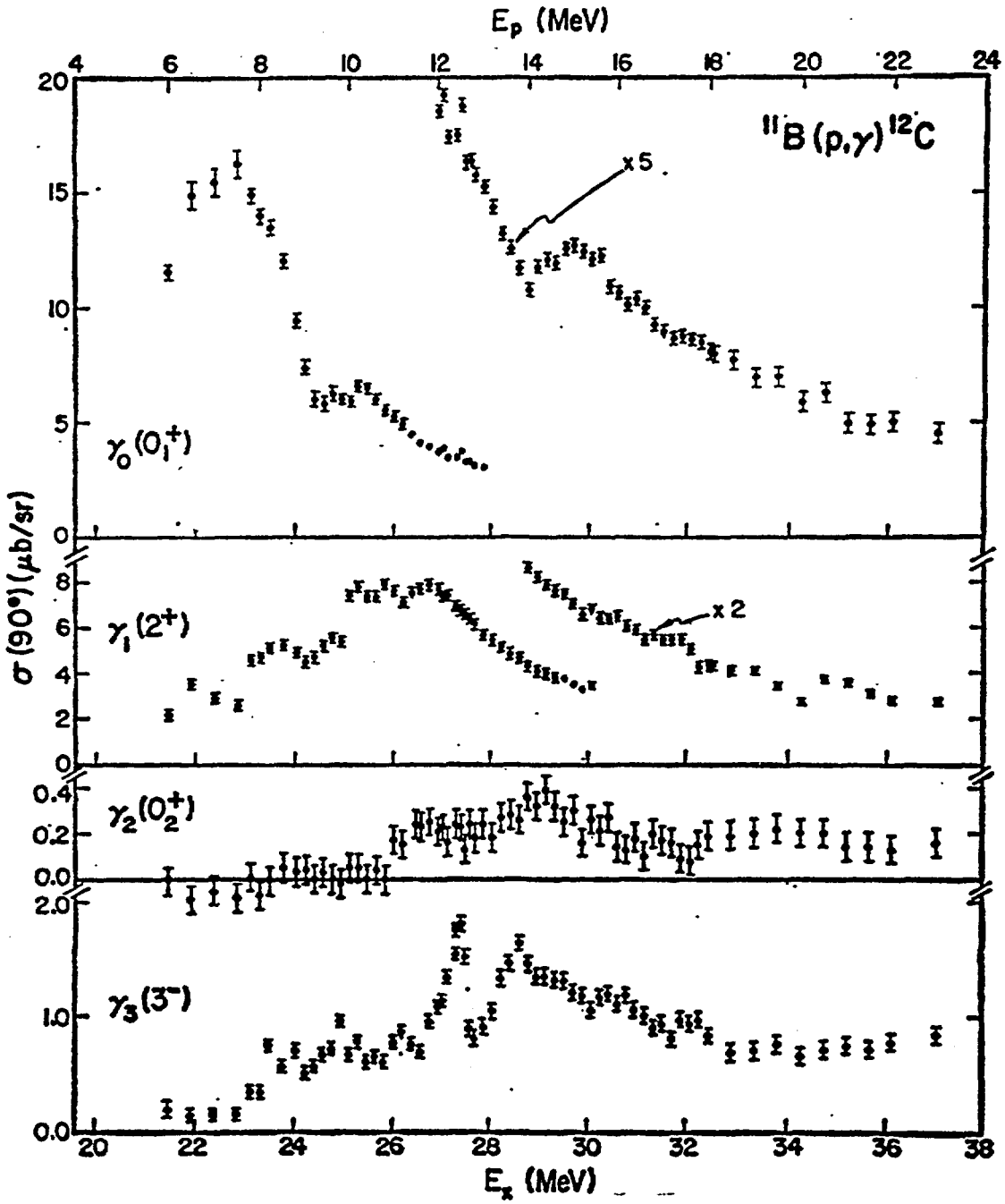

The 90° cross sections for the $^{11}B(p,\gamma)^{12}C$ reaction for transitions to the lowest-four energy levels in ^{12}C as a function of excitation energy (lower scale) and proton energy (upper scale). The error bars shown are statistical; systematic uncertainties due to the efficiency calibration are estimated to be $\pm \leqq 20$ %. The γ_2 cross section has an additional uncertainty of ± 0.05 μb/sr

and the 90° cross sections for the production of the γ_0 and γ_1-rays measured by [All64],

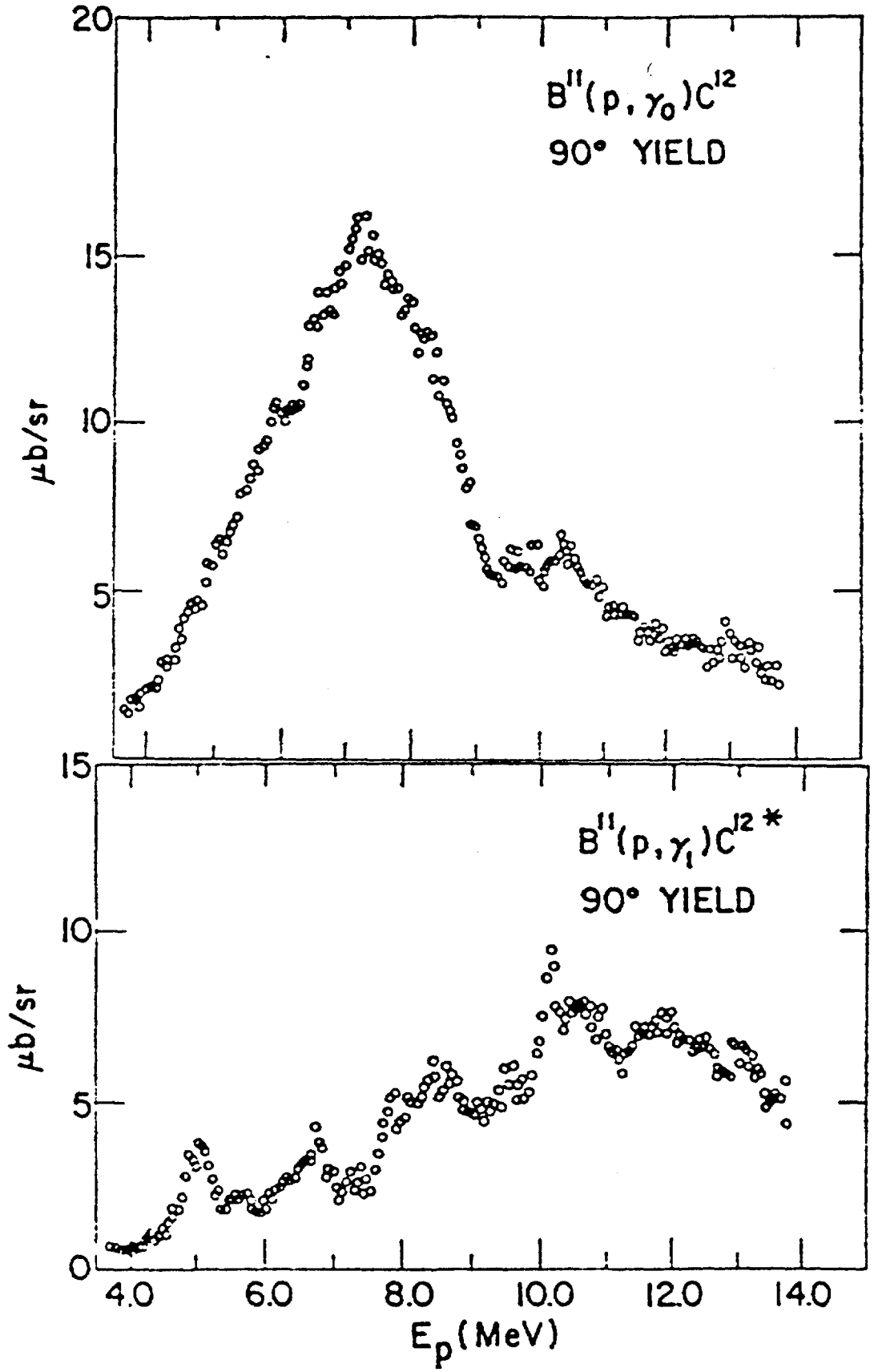

The 90° yield curve in 50 keV steps

2. The $^{12}C(p,p')^{12}C^*$ and $^{12}C(n,n')^{12}C^*$ reactions

The cross sections obtained by measuring of the inelastic groups of nucleons due to excitation of the 4.439 MeV and the 15.11 MeV levels in $^{12}C^*$ are expected not to differ from the ones obtained by detecting the γ-rays that follow the decay of these states formed in inelastic scattering of nucleons. The approximate equality of these cross sections within the experimental errors was verified experimentally for the 4.439 MeV state up to the threshold proton energy E_p=22 MeV of the $^{12}C(p,2p)^{11}B$ reaction, producing the interfering γ-rays of energy 4.44 MeV from the decay of the excitet state in ^{11}B, and for the 15.11 MeV state up to about 27 MeV of incident proton energy (compare e.g. the integral cross sections of [Mea73] and [Sco67]). This equality is due to the fact that the two excitet states in question decay almost entirely by γ-ray emission in agreement with the estimates of [Han60] and [Alm59]. To the contrary most of the remaining excitet states in ^{12}C but the 7.654 MeV and 16.106 MeV states are unstable against break-up into α-particles and therefore show little γ-branchings. At proton energy of 45.5 MeV the overall contribution of the higher excitet states to the 4.44 MeV γ-rays amounts to at least 4.6 mb against the 32.0±1.3 mb populating the 4.439 MeV state (according to the data of [Sat67]).

The differential cross sections for excitation of the 4.439 MeV state in the $^{12}C(p,p')^{12}C^*$ reaction were measured in the proton energy range from 6.65 MeV to 65 MeV [Rei56,Bar66,Dae64,Ger75,Sat67,Del83,Ho78,Kat80] and in the $^{12}C(n,n')^{12}C^*$ reaction at neutron energies 22.0, 24.0 and 26.0 MeV [Ols89,Mei85]. Cross sections for excitation of the 15.11 MeV state were measured via proton scattering at incident energies from 20.5 MeV to 45.0 MeV [Ger75,Sco67].

2.1 The 4.439 MeV state

The first excitet level of ^{12}C at 4.439 MeV decays with a 100% branching to the ground state, emitting the 4.44 MeV γ-rays of multipolarity $E2$. The differential cross sections for inelastic proton scattering into this level was measured by Barnard *et al.* [Bar65] in the proton energy range 6.65 Mev to 11.6 MeV,

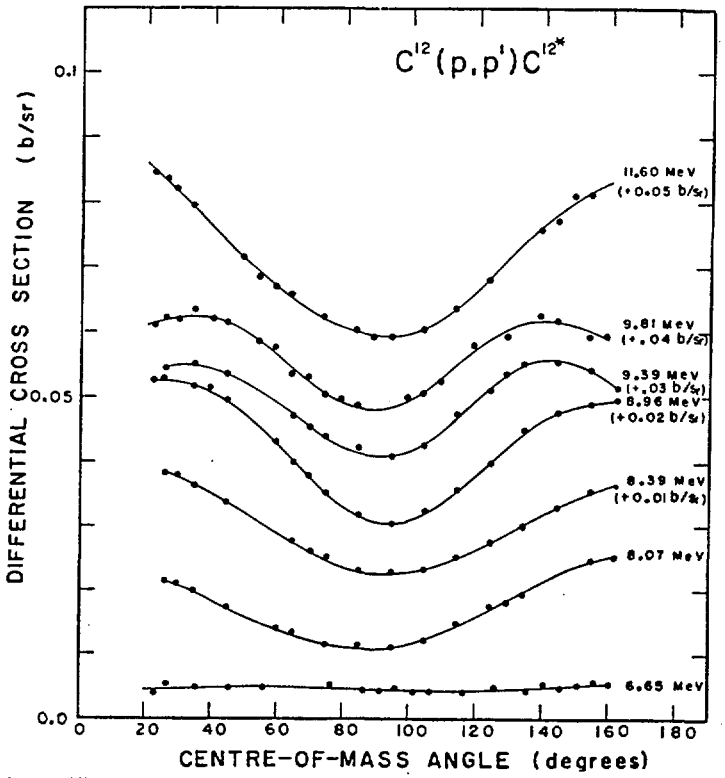

Absolute differential cross sections for the inelastic scattering reaction $^{12}C(p, p')^{12}C^*$ (Q = −4.43 MeV), as a function of angle at the energies shown. The points are the experimental data, and the solid curves were calculated from the Legendre series in table 1. Note that the zero b/sr for the angular distributions has been displaced by the amount given in the parentheses.

These data were described by a series of Legendre polynomials and the resulting expansion coefficients being shown in a numerical form. The integral cross section was evaluated as $4\pi A_0$ with A_0 being the expansion coefficient of the zero-order polynomial.

Coefficients of Legendre series which represent the reaction data (p, p'), (p, p''), and the resulting total reaction cross sections

E_p (MeV)	A_0	A_1	A_2	A_3	A_4	A_5	A_6	A_7	A_8	x^2	σ_T (mb)
					$^{12}C(p, p')^{12}C^*$						
6.65	0.0047	−0.000004	0.0004	−0.0007	−0.00007					0.0051	59
	0.0047	−0.000004	0.0004	−0.0007	−0.00009	0.00001	−0.00008			0.0051	
	0.0047	−0.0001	0.00005	−0.0010	−0.0005	−0.0002	−0.0004	−0.0006	−0.0007	0.0043	
8.07	0.0160	−0.0016	0.0098	0.0002	−0.0004					0.00008	201
	0.0160	−0.0016	0.0098	0.0002	−0.0004	0.0001	−0.0002			0.00008	
	0.0159	−0.0018	0.0095	−0.0002	−0.0009	−0.0003	−0.0007	−0.0006	−0.0005	0.00007	
8.39	0.0187	0.0021	0.0114	−0.0005	−0.0008					0.00003	235
	0.0187	0.0021	0.0114	−0.0005	−0.0008	−0.0001	0.00002			0.00003	
	0.0186	0.0020	0.0111	−0.0007	−0.0012	−0.0004	−0.0004	−0.0001	−0.0007	0.00002	
8.96	0.0206	0.0028	0.0159	−0.0017	−0.0059					0.00004	260
	0.0206	0.0028	0.0159	−0.0017	−0.0059	0.00005	−0.0001			0.00004	
	0.0206	0.0029	0.0160	−0.0016	−0.0058	0.0001	0.000005	0.0002	0.0002	0.00004	
9.39	0.0185	−0.0002	0.0099	0.0007	−0.0079					0.0003	230
	0.0185	−0.0002	0.0099	0.0009	−0.0075	0.0013	−0.0009			0.0001	
	0.0183	−0.0006	0.0094	0.0003	−0.0081	0.0006	−0.0019	−0.0015	−0.0007	0.00009	
9.81	0.0158	0.0002	0.0096	0.0013	−0.0080					0.0011	195
	0.0157	0.0002	0.0095	0.0012	−0.0082	−0.0003	−0.0007			0.0011	
	0.0157	0.0001	0.0095	0.0011	−0.0082	−0.0004	−0.0006	−0.0004	0.0002	0.0011	
11.60	0.0190	0.0004	0.0191	0.0006	−0.0003					0.0006	330 [a]
	0.0189	0.0006	0.0191	0.0007	−0.0003	0.0016	−0.0002			0.0004	
	0.0189	0.0004	0.0187	0.0002	−0.0008	0.0013	−0.0006	−0.0011	−0.0009	0.0003	
					$^{12}C(p, p'')^{12}C^*$						
11.60	0.0012	0.0002	−0.0005	−0.0009	0.0003					0.0074	15
	0.0012	0.0002	−0.0004	−0.0009	0.0001	−0.0081	0.0003			0.0042	
	0.0012	0.0003	−0.0003	−0.0007	0.0003	0.00004	0.0004	0.0002	0.0001	0.0037	

[a]) Includes contribution from $^{12}C(p, p'')$ inelastic scattering and estimate of $^{12}C(p, \alpha_0)$ reaction.

In [Dae64] the differential data were extended over the proton energy range from 14.6 to 19. 6 MeV,

Experimental cross sections for $C^{12}(p,p')C^{12}$ (4.43 MeV) in the laboratory system.
(Angles in degrees, differential cross sections in mb/sr.)

E_{LAB} (MeV) \ ϑ_{LAB}	15°	25°	35°	45°	50°	60°	70°	80°	90°	100°	110°	120°	130°	140°	150°	160°
14.6								7.1	6.1	6.5	8.7	9.5		14.4		
8	58.0	52.0		29.9	25.3	16.5	10.8	7.2	6.0	6.2	7.7	9.7	12.1	13.4	14.3	14.2
15.0		49.3		29.4		17.0		8.0	5.6	5.4	6.7	8.8	11.8	13.2	14.7	14.1
2		46.9		27.1	22.0	16.2	11.5	8.5	6.1	5.4	6.2	8.5	11.9	15.4	17.5	18.4
4	55.3	44.2		25.4		14.7		8.0	6.2	6.4	7.1	9.3	12.0	14.6	16.3	19.6
6		45.1		25.5	21.3	14.8	10.4	7.5	6.0	6.2	7.2	9.5	11.5	13.3	14.7	16.1
8		44.1		25.3		14.2		6.5	5.5	6.0	7.0	8.8	10.5	12.3	12.9	14.0
16.0	50.2	44.4		25.0		13.9	9.0	6.4	5.4	5.8	6.8	8.6	10.0	11.2	12.0	12.8
2		42.6		24.6		13.9		5.9	5.4	5.9	6.6	8.0	9.3	10.5	11.2	12.0
4		41.1	31.7	24.3		13.8	8.7	5.9	5.2	5.7	6.5	7.7	9.0	9.7	10.4	10.8
6		38.3		23.6		13.6		6.1	5.1	5.8	6.5	7.7	8.7	9.5	9.9	10.0
8	38.8	36.6	29.1	23.1		13.9	9.5	6.3	5.2	5.7	6.5	7.9	8.6	9.7	10.5	11.0
17.0	36.9	34.1	27.5	23.4	20.3	14.1	9.5	5.9	4.80	5.1	6.3	7.4	8.5	9.8	10.8	11.7
2		34.3		23.0		13.9		5.8	4.45	5.2	6.1	7.5	8.8	9.8	11.1	12.2
3		32.8	27.3	22.5		13.4	8.4	5.5	4.36	5.1	6.2	7.5	8.9	10.1	11.2	12.4
4		32.4	27.5	21.8		12.8		5.6	4.25	4.85	5.9	7.5	8.7	9.9	10.7	12.3
5		33.0		21.8		12.8			4.25	4.50	5.4	7.0	7.9	9.4	10.3	12.2
17.6	40.2	33.9	26.7	22.5	20.7	13.7	8.8	5.7	4.13	4.14	4.86	6.1	7.3	8.6	9.8	10.9
7		36.1		24.5		14.7				3.95	4.40	5.4	6.3	7.3	8.2	9.4
8		37.3	30.0	24.9		15.1		5.9	4.20	3.80	4.20	5.2	5.9	6.8	7.5	8.5
9		37.0		24.6		15.1	10.0	6.2	4.45	3.90	4.40	5.0	5.8	6.6	7.5	7.8
18.0	38.3	37.6	30.5	24.5	21.2	14.9	9.9	6.2	4.55	4.05	4.55	5.2	5.7	6.6	7.1	7.7
2		34.1		23.6		14.8	10.3	6.3	5.0	4.30	4.65	4.90	5.5	6.2	6.9	7.4
4		32.4	26.1	22.2	19.5	14.0	9.3	6.4	5.1	4.49	4.70	4.87	5.3	5.9	6.5	7.4
6		31.5		21.3		13.1	8.6	5.7	4.90	4.60	4.70	4.85	5.2	5.6	6.2	6.9
8	36.0	32.2	26.3	21.4	18.3	12.7	8.0	5.2	4.64	4.80	4.84	4.91	5.2	5.3	5.9	6.2
19.0	34.2	30.2		20.8		12.5	7.8	4.9	4.45		4.95	4.95	5.2	5.4	5.6	5.7
2	34.0			19.1	17.4	11.5	7.4	5.2	4.34	4.49	4.81	5.0	5.2	5.3	5.7	5.4
4	30.2			18.4			7.2				4.55					5.5
6	34.3			19.2												5.1
Relative error	4%	3%	6%	3%	3%	3%	4%	4%	4%	4%	4%	4%	3%	3%	3%	3%

The differential cross sections for inelastic scattering of protons to the 4.439 MeV level in the projectile energy range from 21.6 MeV to 49.48 MeV were gathered by Sukhovitskij *et al.* [Suk98].

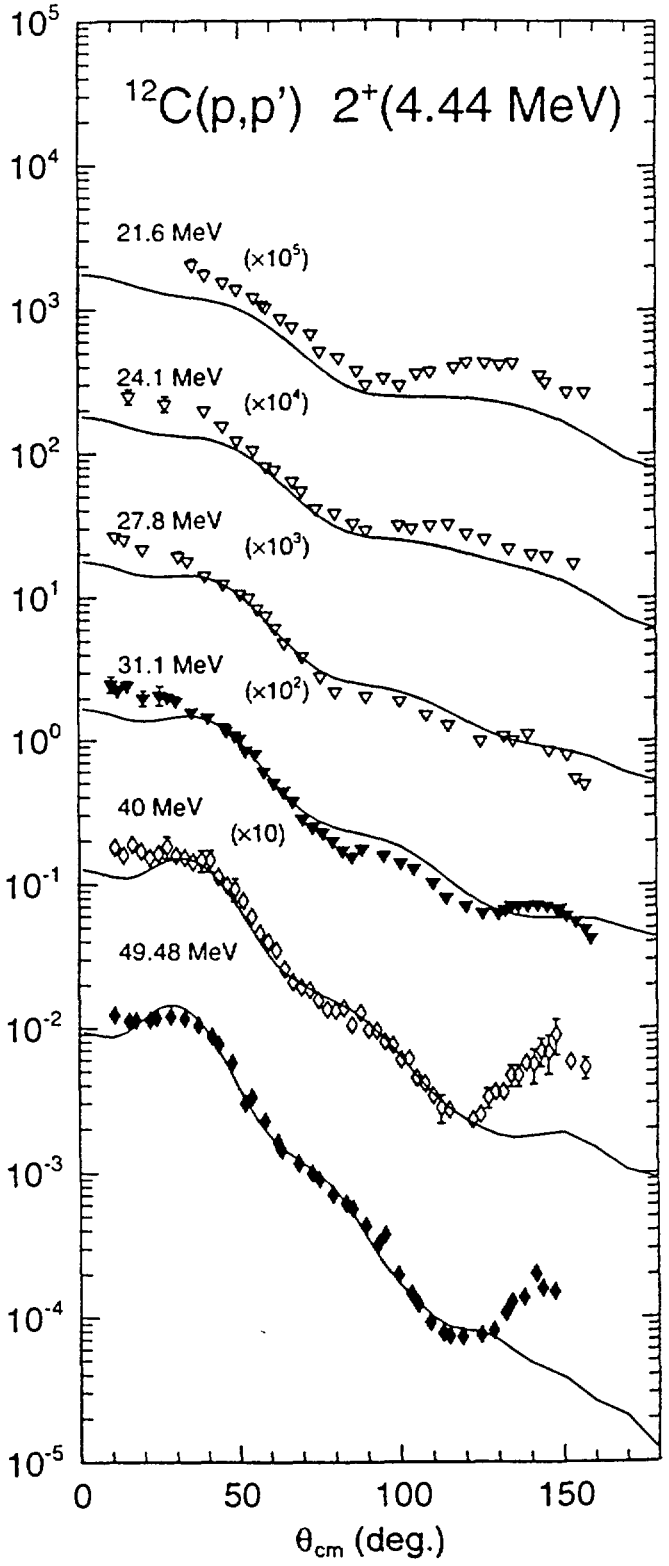

The open-down triangles are from [Dic63], the closed-down triangles are from [Dic63a], the open diamonds are from [Blu66] and the closed diamonds are from [Fan67], respectively.

A few proton angular distributions were measured by Geramb *et al.* [Ger75] with a finer energy step between 30 MeV and 38 MeV (the right hand side figure below) and between 30 MeV and 65 MeV by [Sat67,Leo83,Hos78,Kat80] (the left hand side below),

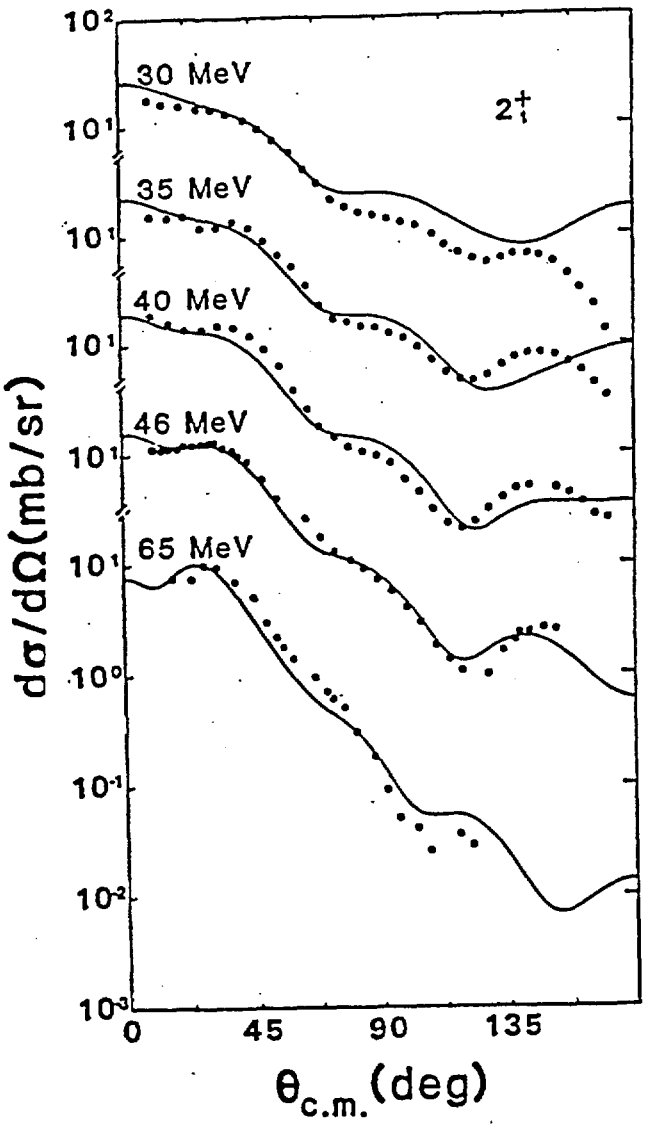

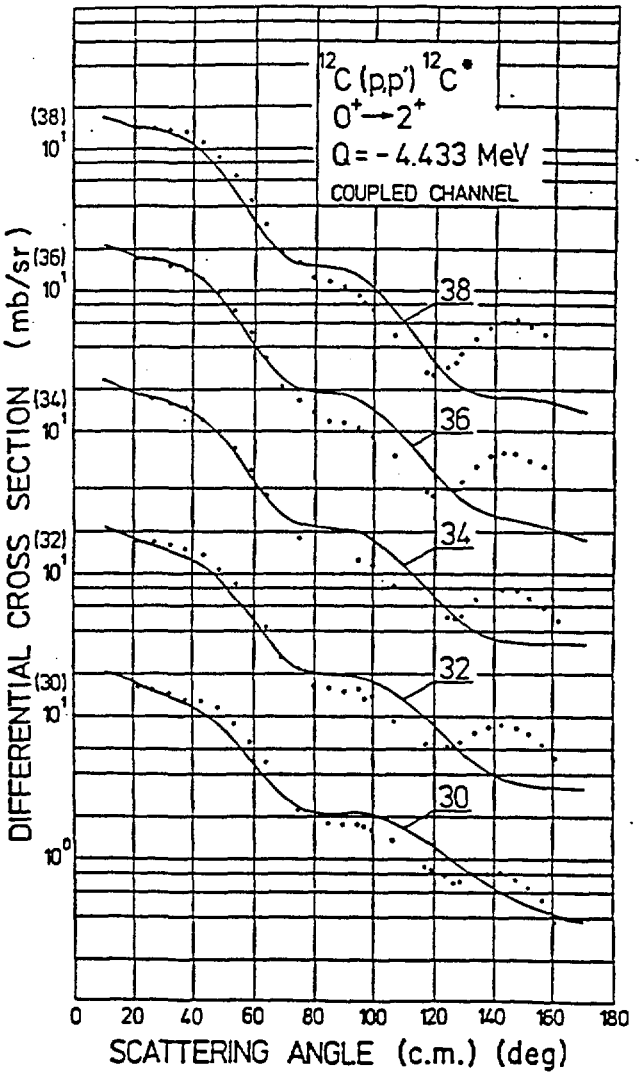

All the differential inelastic cross sections gathered above have no immediate application in a calibration procedure using γ-rays. However, by fitting to Legendre polynomial series they enable extraction of the integral inelastic cross sections that characterize the strenght of the reaction as a γ-ray source. The integral inelastic cross sections can be then compared with the γ-ray production cross section contained in section 3.1 and in conjunction with the angular distribution of the emitted γ-rays can be used already immediately for calibration of a γ-ray detector. It is obvious that as far as the 4.44 MeV γ-rays are concerned the effect of the $^{12}C(p,2p)^{12}C^*$ reaction producing some background γ-rays which can not be easily resolved has to be taken into account (see section 3.1).

The cross sections for excitation of the 4.439 MeV level has been also investigated in the $^{12}C(n,n')^{12}C^*$ reaction. Angular distributions of neutrons have been measured at incident energies 20.8, 22.0, 24.0 and 26.0 MeV [Mei85] as well as at 28.2 MeV [Chi97], as shown below,

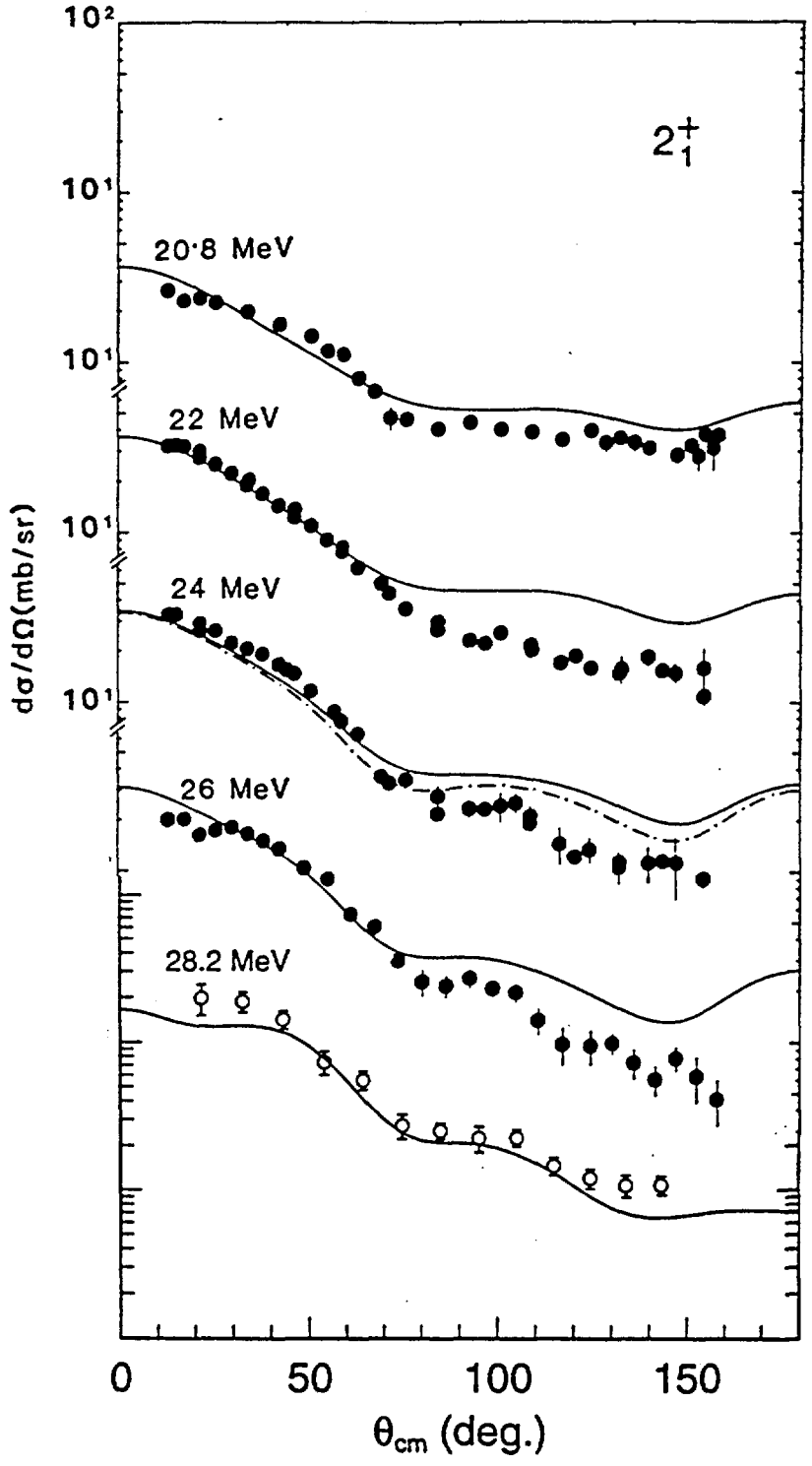

To end with the data for the excitation of the 4.439 MeV level we present the excitation curves measured at six laboratory angles (25.54°, 85.22°, 105.23°, 121.16°, 137.52° and 159.45°) by Swint *et al.* [Swi66] as well as the six-angle-integrated excitation curve [Bar66], which can be used together with the angular distributions of γ-rays following inelastic scattering of [Zob68,Dye81] (see section 3.1) when low energy protons are applied for detector calibration. As shown in the sequel these excitation curves cover the energy range from 6.7 to 11.5 MeV.

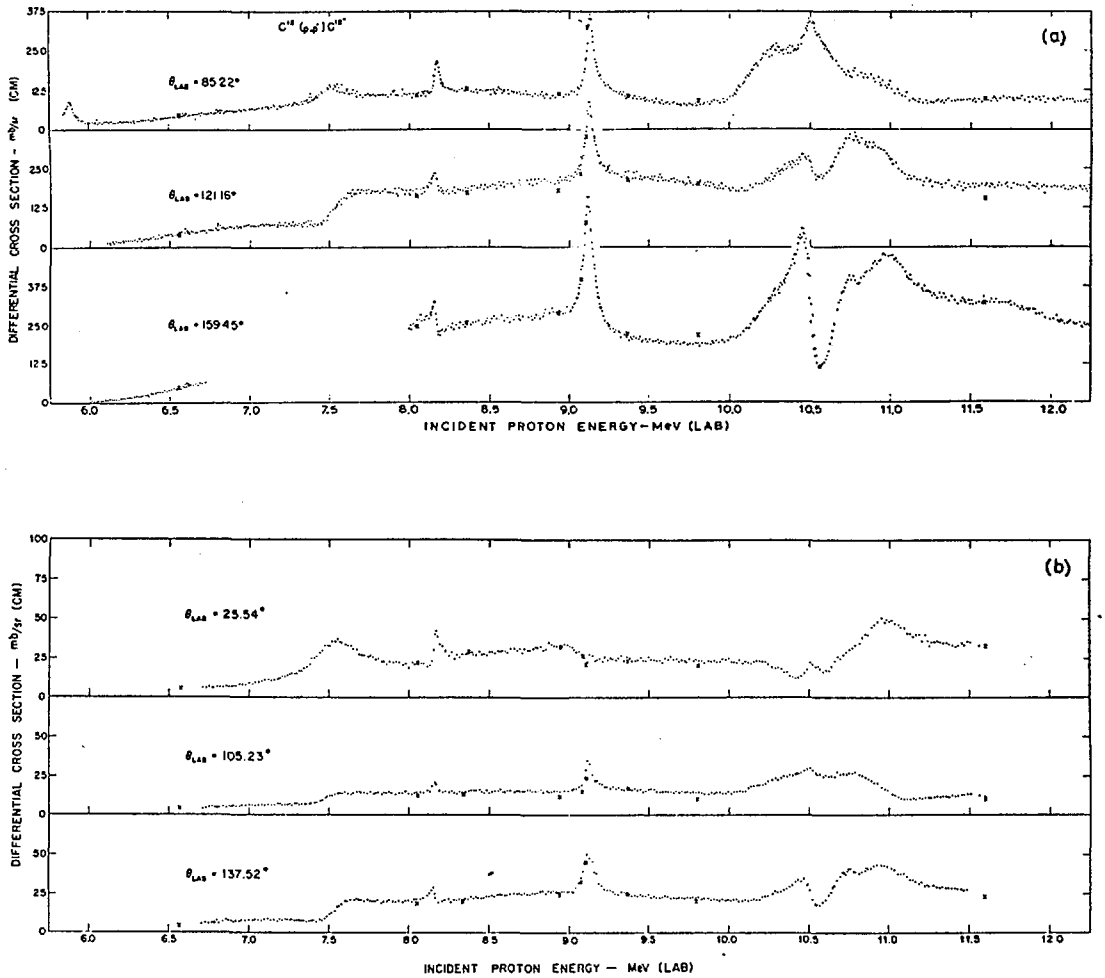

Fig. 2. a, b. Excitation functions for the inelastic scattering reaction $^{12}C(p, p')^{12}C^*(Q = -4.43$ MeV). The dots represent the experimental points. Only every second point was plotted except over narrow resonances. Angular distribution points are plotted as ×. A small correction should be made to the energy scale: the points are plotted at energies too low by 0.25%. The excitation functions in fig. 2a continue uneventfully to 12.8 MeV.

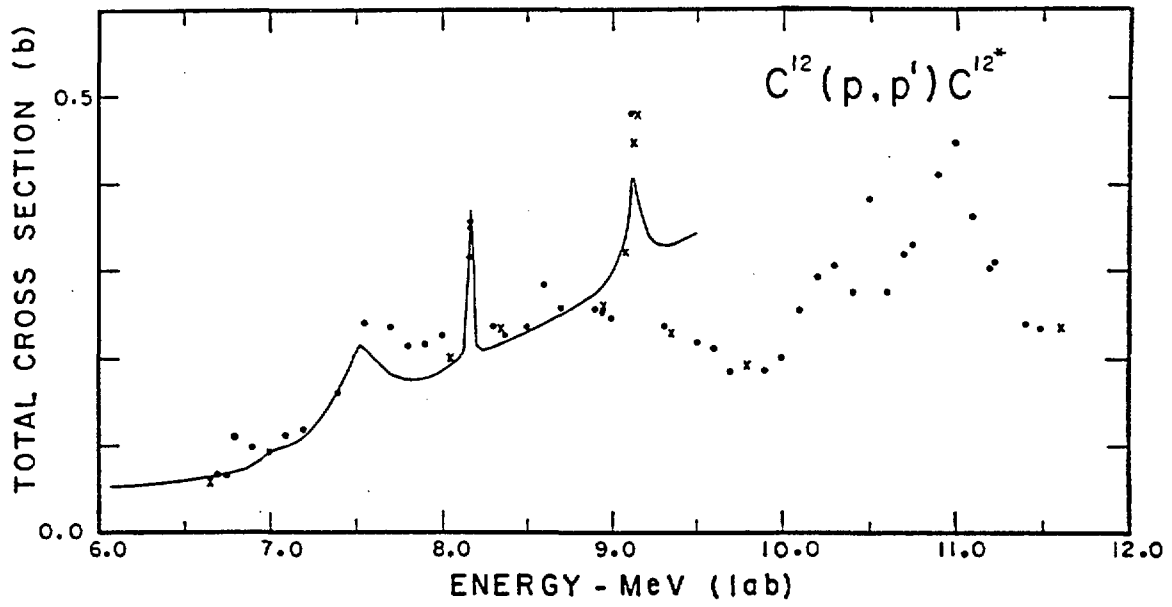

Estimates of total cross sections for the $^{12}C(p, p')^{12}C^*$ ($Q = -4.43$ MeV) reaction

The crosses correspond to the integral data from the Table given at the beginning of the present chapter.

2.2 The 15.11 MeV state

The angular distributions of the inelastic proton groups to the 15.11 MeV level in ^{12}C have been investigated by [Sco67] in the incident proton energy range from 20.5 MeV to 30.25 MeV, as well as by [Ger75] at proton energies from 22.5 MeV to 45 MeV. These data are displayed in the figures that follow,

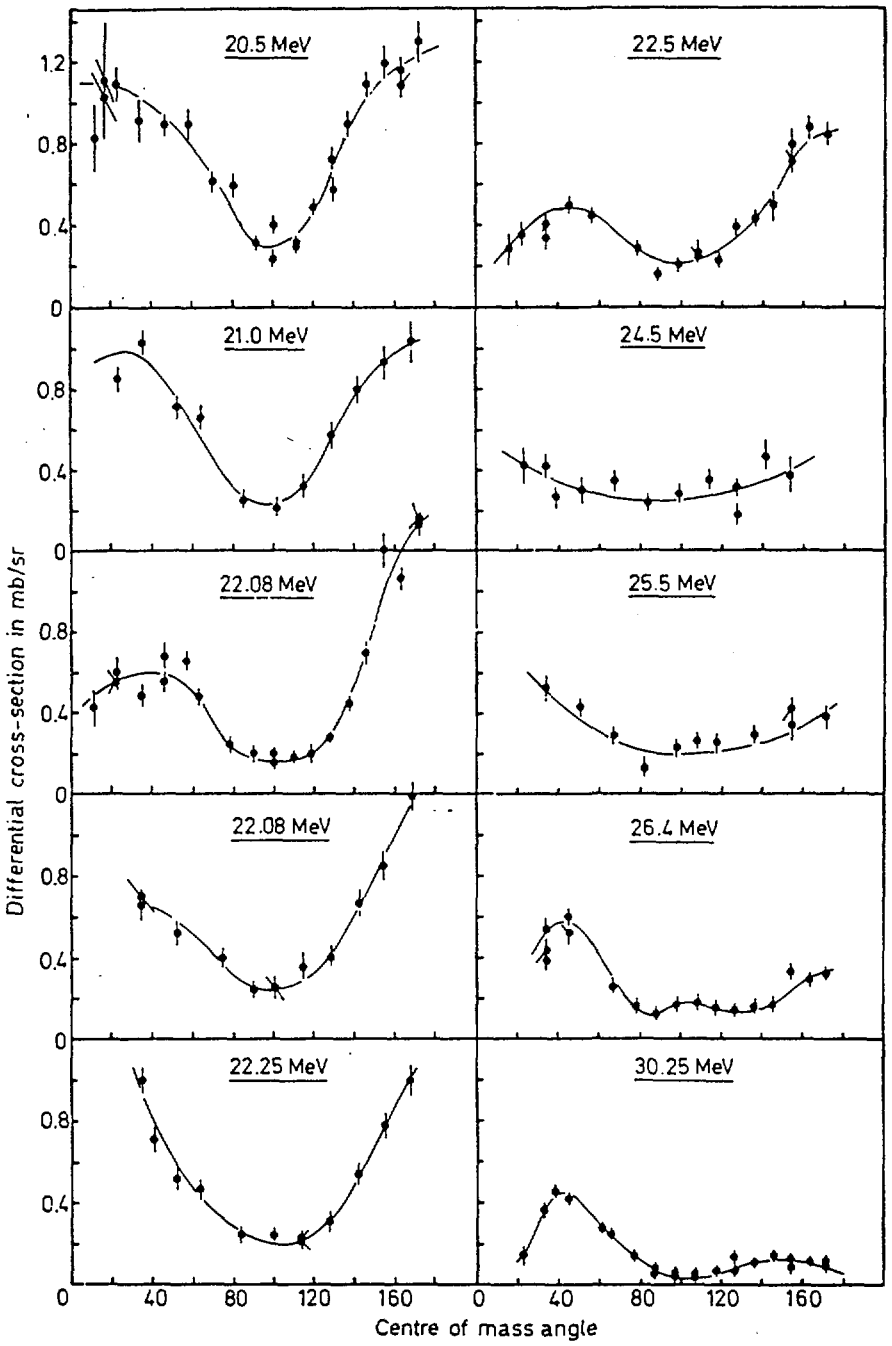

Angular distributions of inelastic protons for the reaction $^{12}C(p, p')^{12}C^*$ (15.11 MeV, 1^+, $T = 1$).

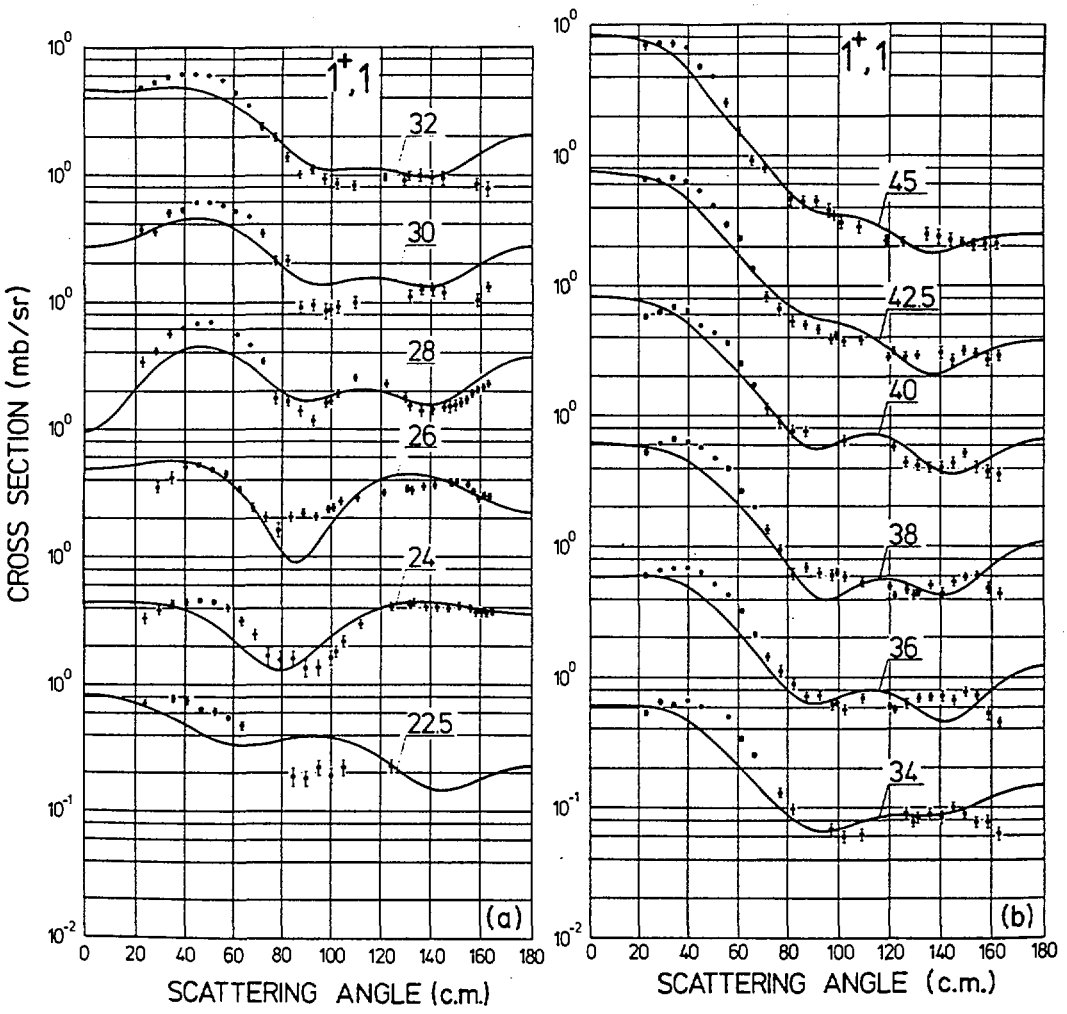

(a) Differential cross sections for inelastic proton scattering to the 1^+ $T=1$ (15.11 MeV) state in ^{12}C for projectile energies between 22.5 and 32 MeV. (b) Differential cross sections for inelastic proton scattering to the 1^+ $T=1$ (15.11 MeV) state in ^{12}C for projectile energies ranging between 34 and 45 MeV.

The integrated cross sections derived in [Sco67] by integrating Legendre fits to the data are given in Table that foolows.

Integrated cross sections for the reaction $^{12}C(p, p')^{12}C^*$ (15.11 MeV, 1^+, $T = 1$ level)

E_{lab}(MeV)	σ(mb)	$\Delta\sigma$
20.5	8.58	0.75
21.0	7.09	0.75
22.08	5.93	0.75
22.08	5.32	0.75
22.25	5.93	0.75
22.5	4.69	0.45
24.5	3.76	0.75
25.5	4.05	0.75
26.4	3.62	0.75
30.25	1.60	0.44

The errors are estimated from the statistical goodness of fit.

The angular distributions of the inelastic proton group exciting the 15.11 MeV level [Ger75] have been integrated by Legendre fits in framework of the present evaluation. The integral cross sections obtained in *mb* are: 4.41±0.56, 3.20±0.32, 3.01±0.32, 2.75±0.30, 2.70±0.36, 2.38±0.25, 2.34±0.25, 2.10±0.21 and 1.94±0.29 at incident proton energies, 22.5, 30, 32, 34, 36, 38, 40, 42.5 and 45 MeV, respectively. These cross sections extend far beyond the content of the Table given above as well as beyond the the set of the A_0 expansion coefficients displayed in section 3.2 .

3. The $^{12}C(p,p\gamma)^{12}C^*$ reaction and comparison with the $^{12}C(p,p')^{12}C^*$ reaction

Due to the exceptionally weak γ-branchings of excited states in ^{12}C, other than the 4.439 MeV and the 15.11 MeV states, the cross sections for inelastic scattering determined via detection of either the γ-rays or the scattered projectiles do not differ within typical experimental errors. The practical equality of these cross sections was verified experimentally, e.g. the inelastic cross sections to the 4.44 MeV level at 12 MeV incident energy determined by integrating the angular distribution of scattered protons was found to be 267±14 mb, in good agreement with the cross section for γ-ray production, which had been found to be 262±26 mb [Dye81].

Erlier experiments used Na(J) crystal as γ-ray detectors. Sample γ-ray spectra from ^{11}B and ^{12}C bombarded with 33 MeV and 16 MeV protons, respectively, detected in a central Na(J) crystal surrounded by two larger Na(J) crystals and operated as an anticoincidence spectrometer are shown after [Zob68],

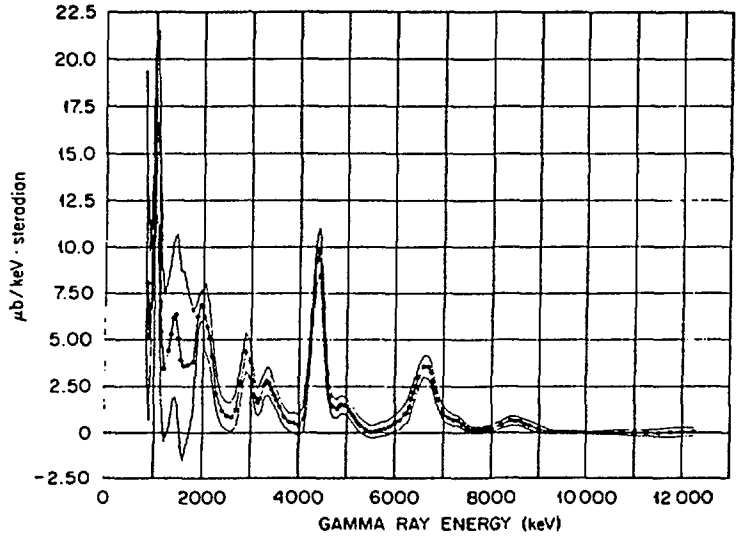

Gamma-ray spectrum at 135° for 33-MeV protons incident on ^{11}B.

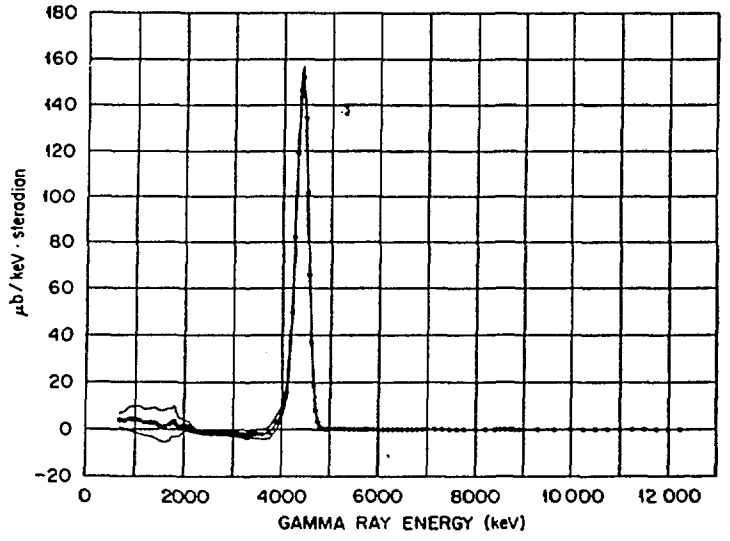

Gamma-ray spectrum at 135° for 16-MeV protons incident on C.

Since in newer experiments Ge(Li) detector are commonly used we present below also a γ-ray spectrum measured with use of a Ge(Li) detector at a proton energy of 15 MeV [Dye81]. In the case of the 4.44 Mev γ-rays, the line shape for photopeak was quite broad, especially for the higher energy incident protons. This is due to events Doppler-shifted to higher energies. The tripled lines correspond to the double-escape-, the single-escape- and the photo-peak.

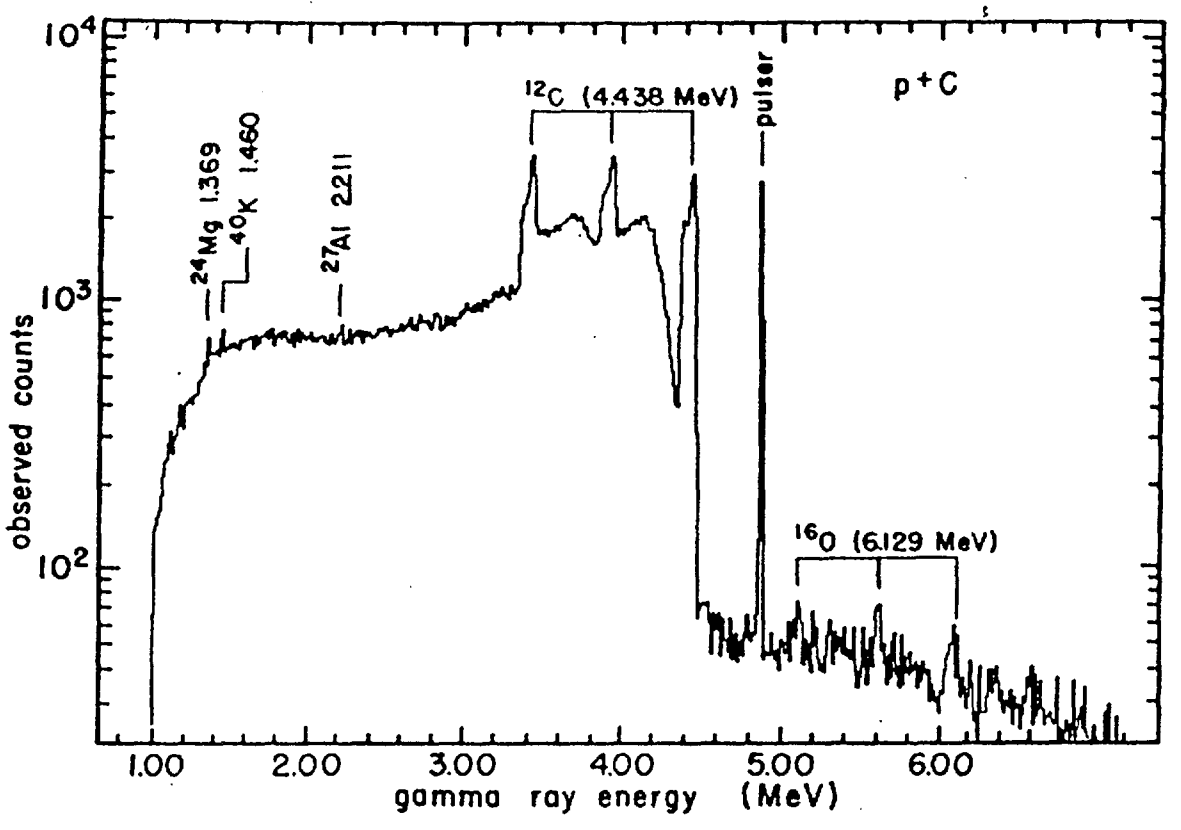

The vertical lines are located at energies corresponding to γ-ray emission energies, uncorrected for Doppler shifts arising from motion of the excited ^{12}C nucleus. Contaminant lines are indicated which arise from oxygen in the target, room background, and proton interaction with the aluminum walls of the scattering chamber.

At proton energies in excess of 16.8 MeV a peak in the γ-ray spectrum arises that can be ascribed to the 15.11 MeV γ-rays from the 15.11 MeV excitet state of ^{12}C, populated in the inelastic scattering followed by γ-deexcitation [Mea63]. The approximate equality of the cross sections for production of the 15.11 MeV γ-rays with the cross sections for formation of the 15.11 MeV state obtained by detecting the inelastic proton group shows that there are no significant γ-transitions to this state from higher excitet states as well as that the 15.11 MeV state decays almost entirely by γ-ray emission in agreement with the decay-scheme shown at the begining of this report [Led78,Fir96]. Typical γ-ray spectra detected in large Na(J) crystals operating in anticoincidence mode with a scintillating shield show the clear separation between the primary capture γ-rays leading to states of ^{13}N and the 12.71 MeV and 15.11 MeV γ-rays that follow inelastic scattering to states of ^{12}C.

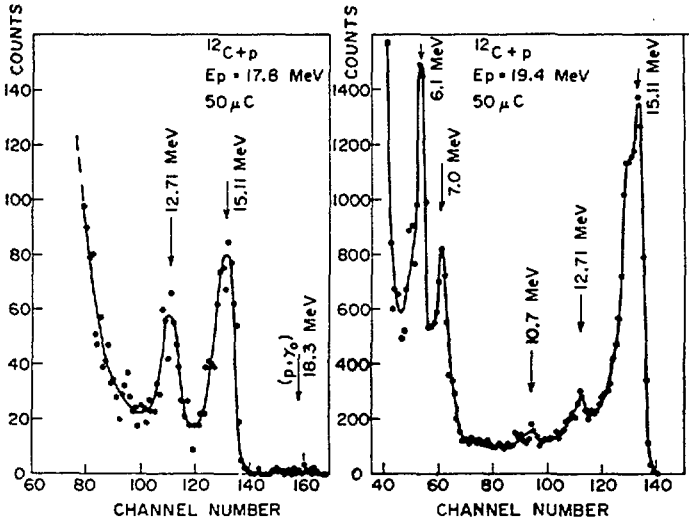

FIG. 3. Gamma-ray spectra for proton energies of 17.8 and 19.4 MeV; note the change in scale of a factor of 10. The 10.7 MeV γ ray comes from the cascade from the 15.11 to the 4.44 MeV level.

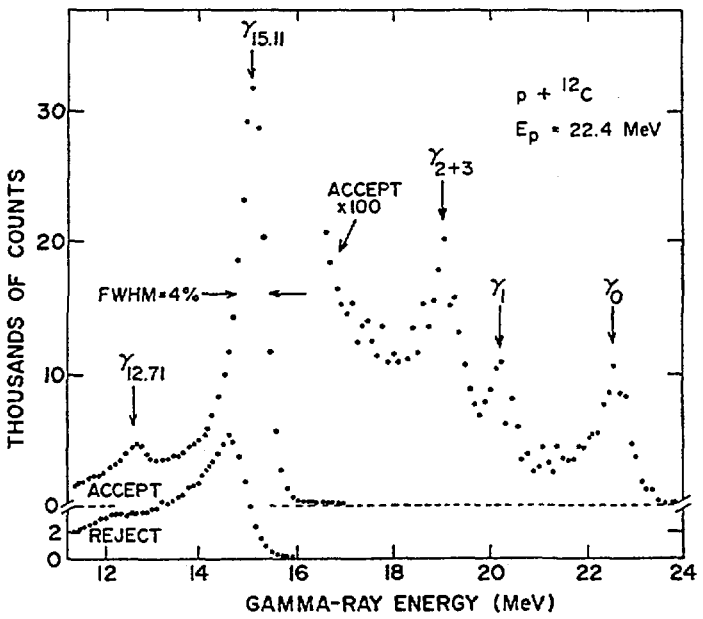

Typical γ-ray spectrum showing the clear separation between the capture γ-rays leading to the ground and excited states of ^{13}N. The "accept" ("reject") spectrum corresponds to events which are in coincidence (anti-coincidence) with the plastic shield which surrounds the NaI

3.1 The 4.44 MeV γ-rays

Cross sections for production of the 4.44 MeV γ-rays in some of the listed reactions were evaluated by Ramaty, Kozlovsky and Lingenfelter [Ram79], and are shown in the sequel. The threshold for excitation of the 4.439 MeV level in ^{12}C is 4.81 MeV and 5.92 MeV for incident protons and α-particles, respectively.

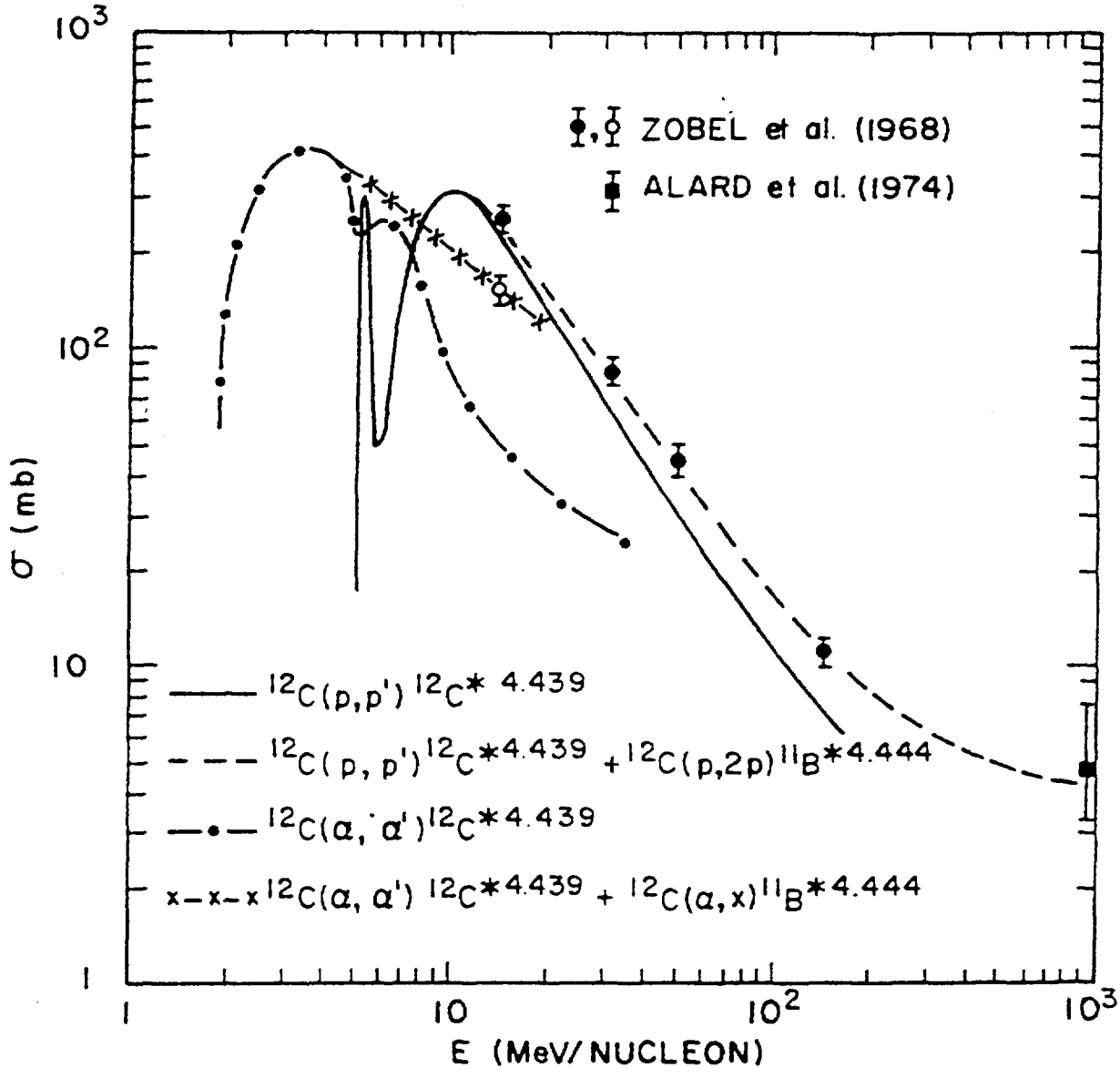

—Cross sections for 4.44 MeV photon production from ^{12}C. *Solid and dot-dashed curves*, direct excitation of the 4.439 MeV level in (p, p') and (α, α') reactions. *Dashed and dash-crossed curves*, total production of 4.44 MeV photons by protons and α-particles, respectively.

The filled circles and the square are production cross sections of the γ-rays of 4.44 MeV resulting from the bombardment of ^{12}C with protons [Zob68, Ala74]. The circles were deduced by using the differential cross sections at 135° and the angular distributions taken at three angles [Zob68]. These cross sections can be compared with the cross sections of the $^{12}C(p,p')^{12}C^*$ reaction

compiled from [Rei56,Bar66,Con57,Dae64,Dic63,Sto64,Fan67,Hor70Emm66,Tyr57] into the solid curve. In the light of what was said above the difference between the γ-ray production data (dashed line) and the (p,p') data (solid line) is assumed to be due to the excitation of the 4.444 MeV level in ^{11}B by the (p,2p) reaction relevant above the 22 MeV threshold.

The cross sections for the $^{12}C(\alpha,\alpha')^{12}C^*$ reaction (dot-dashed curve) are based on measurements between 1.5 and 4.3 MeV per nucleon [Mit64], and at 4.6 MeV [Cor59] and 10 MeV per nucleon [Yav59]. The open circle at 13 MeV per nucleon is a γ-ray production cross section from [Zob68]; thus it includes the contribution from the $^{12}C(\alpha,\alpha'p)^{11}B$ reaction. The dash-crossed curve is an estimate of the sum of the cross sections for both reactions above 5 MeV per nucleon.

The angular distribution data of [Zob68] used in deducing the integral cross sections shown above are gathered in the table that follows,

Angular Distribution of Gamma Rays Produced by Protons and Alpha Particles

Target	$\bar{E}_p$ [a]	$\bar{E}_\gamma$ [b]	$R\frac{90}{135}$ [c]	$R\frac{50}{135}$ [d]
Be	14.7	3460	1.04 ± 0.39	
	14.7	6180	0.86 ± 0.47	
C	50.3	4410	0.90 ± 0.08	
	50.3	~6600	0.89 ± 0.18	
C	32.3	4410	0.94 ± 0.08	0.68 ± 0.08
	32.3	~6600	1.40 ± 0.26	1.16 ± 0.27
C	14.5	4410	0.23 ± 0.03	0.13 ± 0.02
C	[56.3]	4410	0.91 ± 0.08	1.50 ± 0.11
	[56.3]	5250	0.81 ± 0.20	1.48 ± 0.36
	[56.3]	~6600	0.83 ± 0.11	1.21 ± 0.19
O	12.1	6220	0.80 ± 0.10	
	12.1	7080	0.95 ± 0.13	
Al	14.4	2240	0.83 ± 0.17	1.05 ± 0.18
	14.4	2960	0.86 ± 0.17	0.96 ± 0.20

[a] $\bar{E}_p$ = average proton energy in target in MeV. Values in brackets refer to incident alpha particles.

[b] E_γ = approximate gamma-ray energy in keV.

[c] $R\frac{90}{135}$ = ratio of gamma-ray production cross section at 90° to that at 135°.

[d] $R\frac{50}{135}$ = ratio of gamma-ray production cross section at 50° to that at 135° except that the measurement 32.3 MeV was made at 60°

These data are not self-consistent since (we recall) the angular distributions must be symmetric about 90°. In case of the interaction of 14.6 MeV protons with ^{12}C, yielding the 4.44 MeV γ-rays, differential cross sections 2 times smaller (than above) at 135°, about the same at 90°, and 3.5

times larger at 50°, were obtained by Dyer *et al.* [Dye81]. The angular distributions measured in [Dye81] are symmetric with respect to 90°,

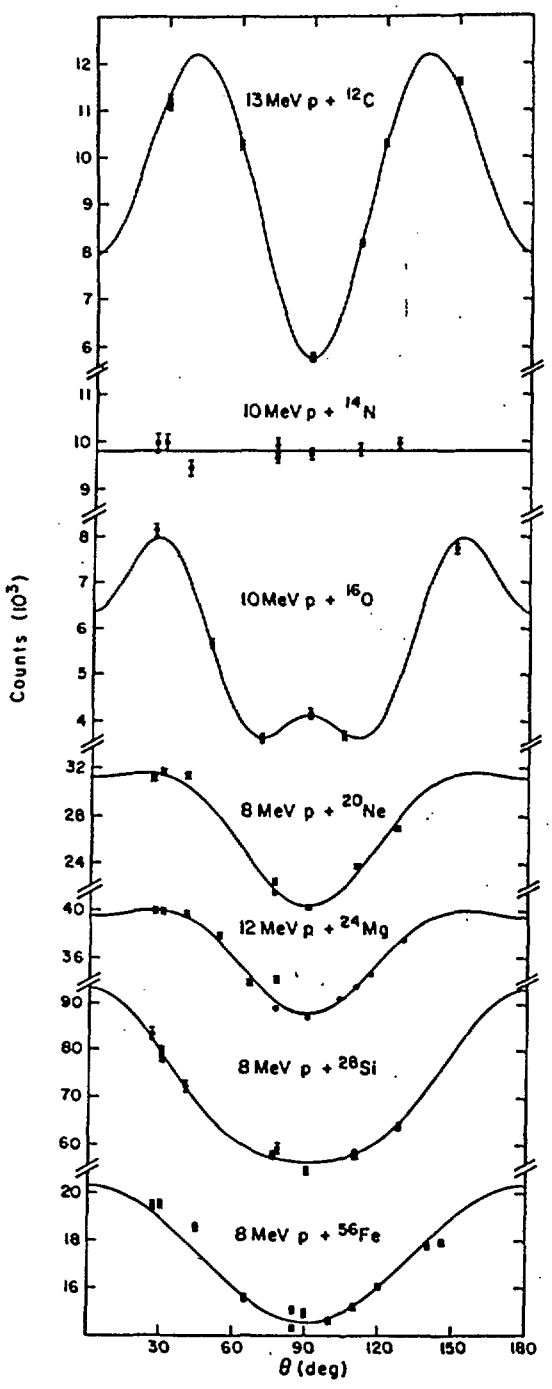

Examples of angular distributions of gamma rays. The solid curves are fits with an expansion in Legendre polynomials of even order through zero for the ^{14}N case, through 6 for the ^{16}O case, and through 4 for the other cases. The gamma-ray energies (top to bottom) are 4.44, 2.31, 6.13, 1.63, 1.37, 1.78, and 0.847 MeV.

The cross sections for the spallation reaction on ^{16}O taken from [Zob68, Ala74] are shown by the curve labelled 1 (see the figure that follows) for incident protons and 6 for α-particles. The latter curve is an estimate based on the single cross section measured at 13 MeV per nucleon. The former has been normalized to the measurements of a (p,αp) reaction on ^{24}Mg [Dye81].

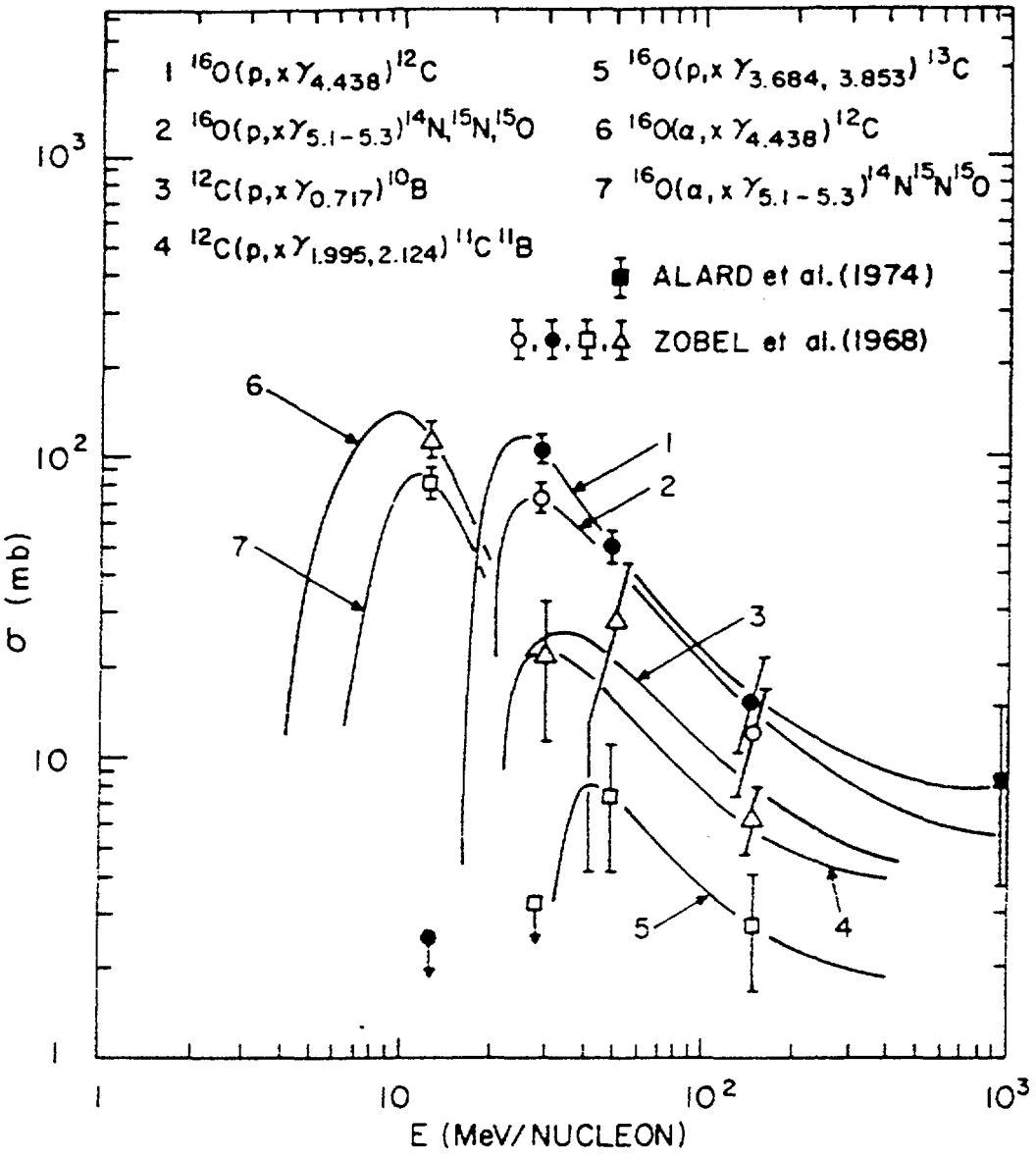

—Gamma-ray production cross sections in spallation reactions of protons and α-particles on ^{12}C and ^{16}O.

For proton spallation of ^{14}N the cross section measured at 120 MeV [Cle61] was used to estimate that the 4.438 MeV γ-ray production cross section from ^{14}N is larger than from ^{16}O by about a factor 2.4 .

Dyer *et al.* [Dye81] give the cross sections for production of the 4.44 MeV γ-rays in more detailes as shown in the following figure,

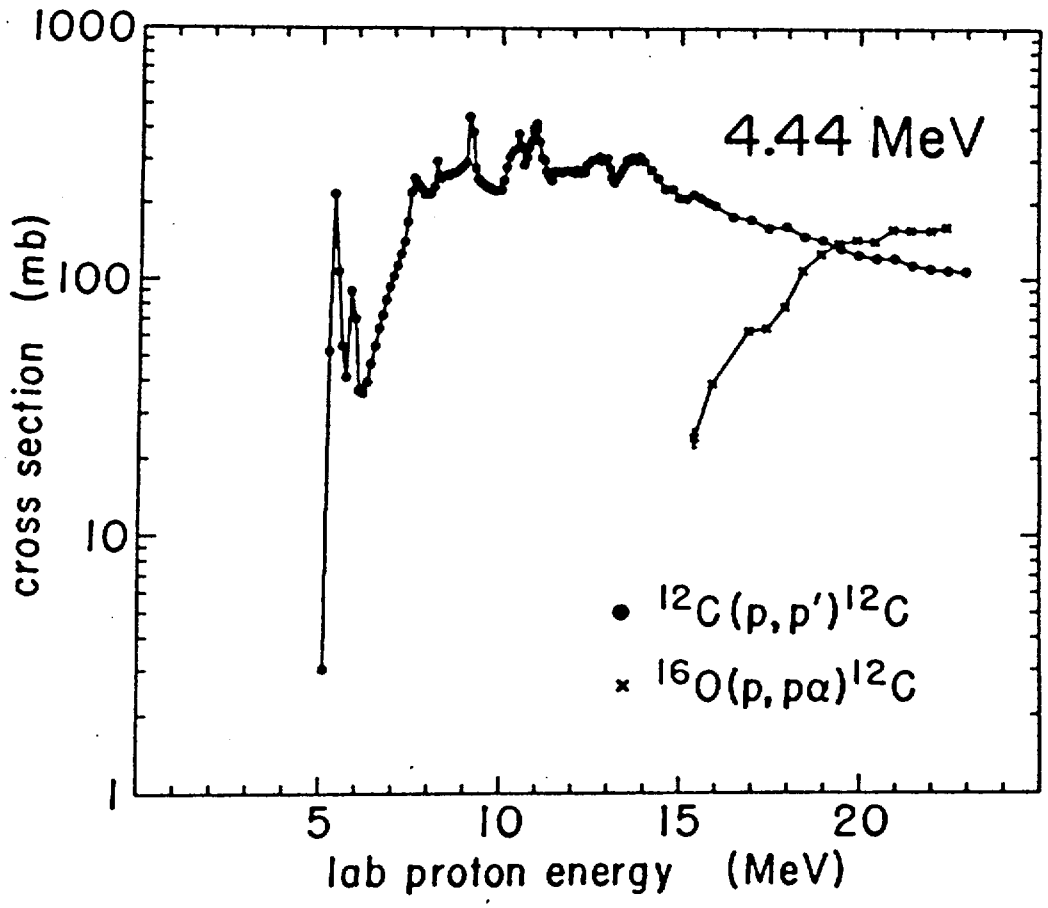

Cross sections for production of 4.44-MeV gamma rays from $p + {}^{12}C$ and $p + {}^{16}O$ reactions. [Note: the delayed contribution from (p,n) reactions followed by β^+ decay is included, when present.]

The cross sections for the $^{12}C(p,p\gamma)^{12}C^*$ reactions include the delayed contribution from the (p,n) reaction followed by β^+ decay. The cross sections averaged over 1 MeV wide energy bins are also available from [Dye81] as numerical data gathered in the table that follows,

Cross sections (in mb) for the production of the 4.44 MeV γ-rays

Target nucleus	^{12}C	^{16}O
Residual nucleus	^{12}C	^{12}C
E_γ (MeV)	4.44	4.44
Beta decay included?	Yes	
E_p=2 MeV		
3		
4		
5		
6	55	
7	108	
8	240	
9	290	
10	265	
11	317	
12	270	
13	282	
14	281	3
15	217	16
16	193	40
17	169	64
18	156	85
19	140	123
20	125	140
21	118	150
22	110	156
23	107	157

3.2 The 15.11 MeV γrays

The 90° cross sections for the 15.11 MeV γ-rays from ^{12}C bombarded with protons were measured by [Ber76], from the threshold energy at 16.39 MeV to 24.4 MeV. The uncertainty in absolute normalization is ±20%. These results duplicate quite well the results of earlier measurements by [Sno68] and [Mea73]. The latter paper presents the 90° excitation function for the 15.11 MeV γ-rays in the incident proton energy range from threshold to 48.5 MeV. The same cross sections were remeasured again from threshold to 24 MeV by [Mea73]. In the threshold region the old data of [War62] are also available. All these data sets are consistent in magnitude but differ in the energy resolution of the proton projectiles and the projectile energy grid. Below the data of [Ber76] are shown. This paper contains also the Legendre polynomial expansion coefficients for the angular distributions of the 15.11 MeV γ-rays. Since the scattered protons are not observed the angular distributions of the measured γ-rays are averaged over the directions of emitted protons and must be symmetric, i.e. only even Legendre polynomials contribute.

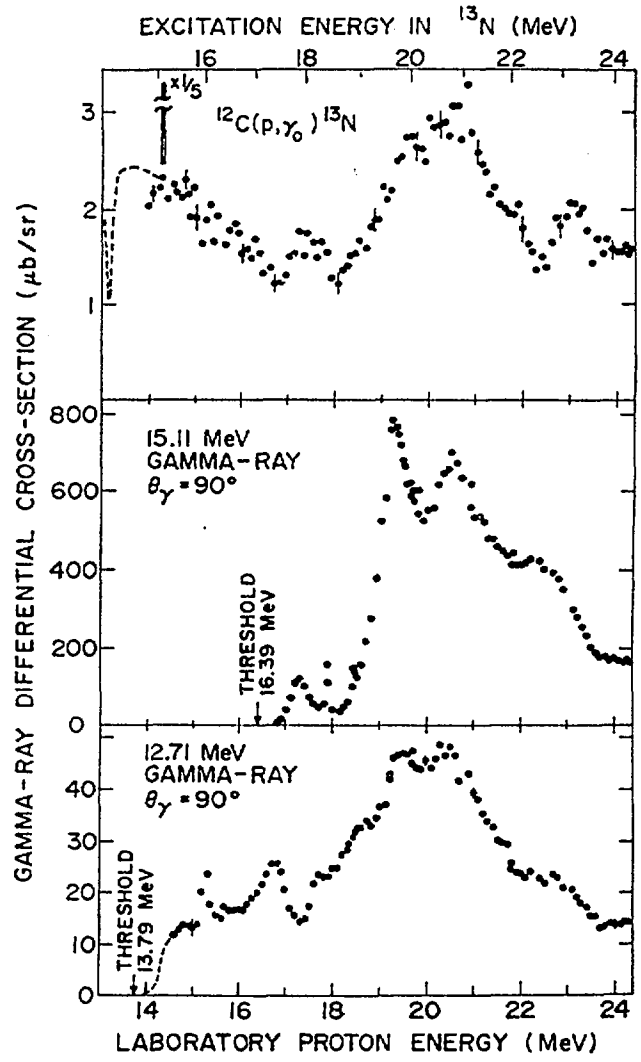

Differential cross section for the 90° yield of the ground-state capture γ-rays together with the 90° yield of the 12.71 and 15.11 MeV γ-rays which result from proton inelastic scattering off ^{12}C. The dashed line in the 12.71 MeV cross section represents the threshold data of Measday *et al.* In addition to the small relative errors, there is an uncertainty on the normalization of ±20 %.

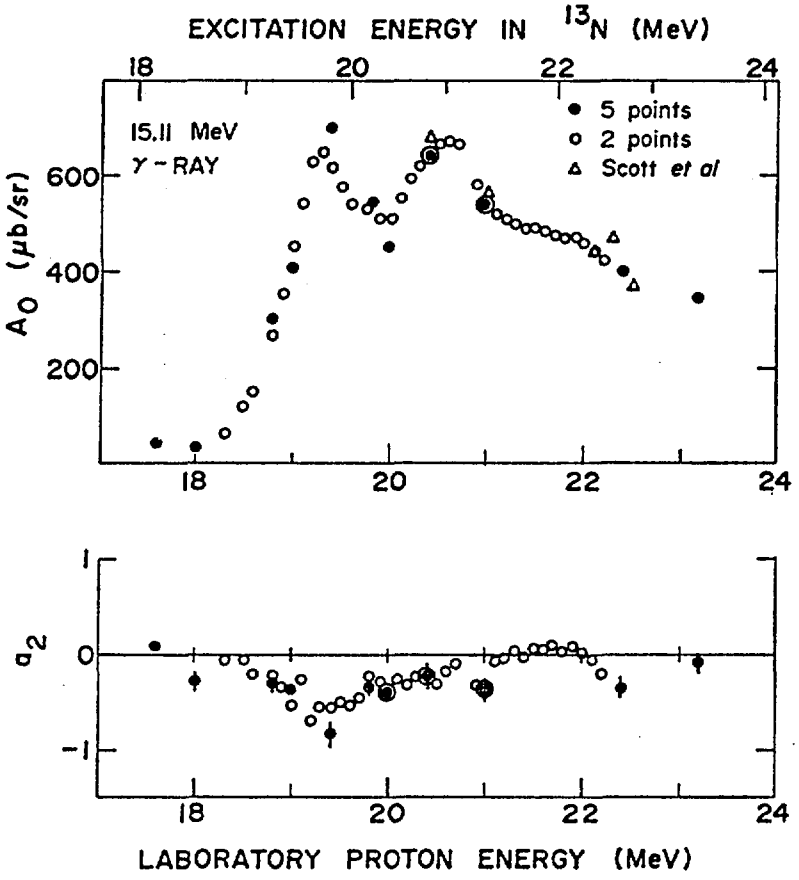

Coefficients of the Legendre polynomials for the angular distributions of the 15.11 MeV γ-ray; the inelastically scattered proton is not observed, so the coefficient a_1 is set equal to zero. The full circles are the results obtained from a five-point angular distribution and the open circles are calculated using $\theta_\gamma = 55°$ and 90° yield curves. The triangles are the total inelastic proton cross sections to the 15.1 MeV state obtained by Scott *et al.*

In the analysis of the angular distributions only A_0 and a_2 were extracted since a_1=0 was found consistent with the cross sections measured at two angles, 55° and 90°, only (open circles). These results were further verified by fitting the five-points angular distributions at chosen proton energies (full circles). The A_0's from the γ-ray production cross sections are compared with the inelastic scattering data of [Sco67] (open triangles). The good agreement (of triangles and circles) corroborates the estimated equality of the cross sections for production of the 15.11 MeV γ-rays and the inelastic cross section to the 15.11 MeV level in ^{12}C.

The earlier data of [Mea73] and [Mea63] are also shown,

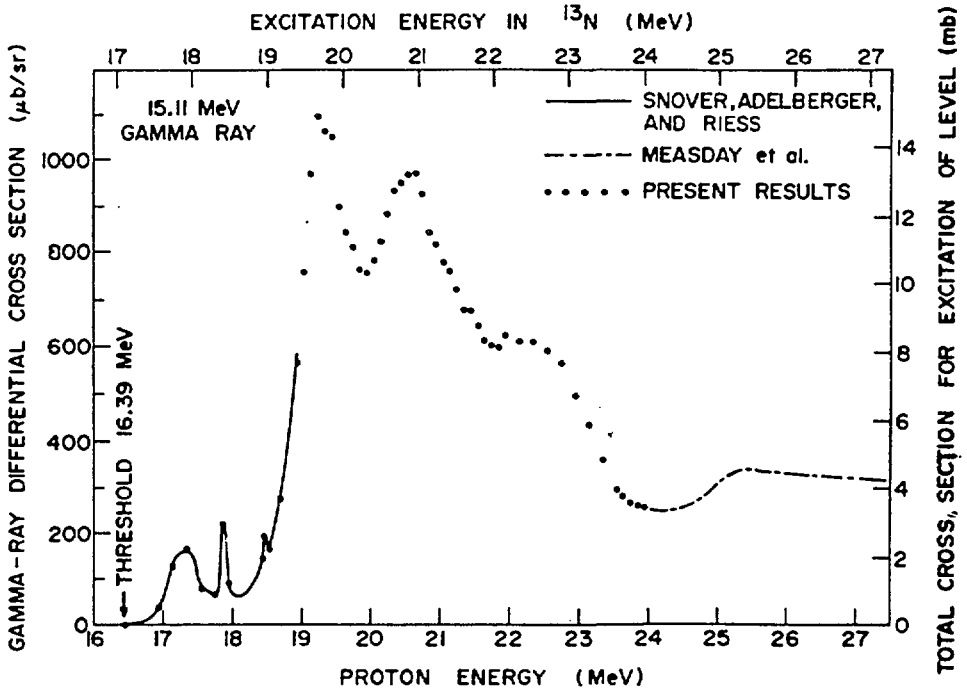

The 90° yield curve for the 15.11 MeV γ ray in proton–carbon collisions. The errors shown are purely statistical and do not include a ±25% uncertainty in the absolute normalization.

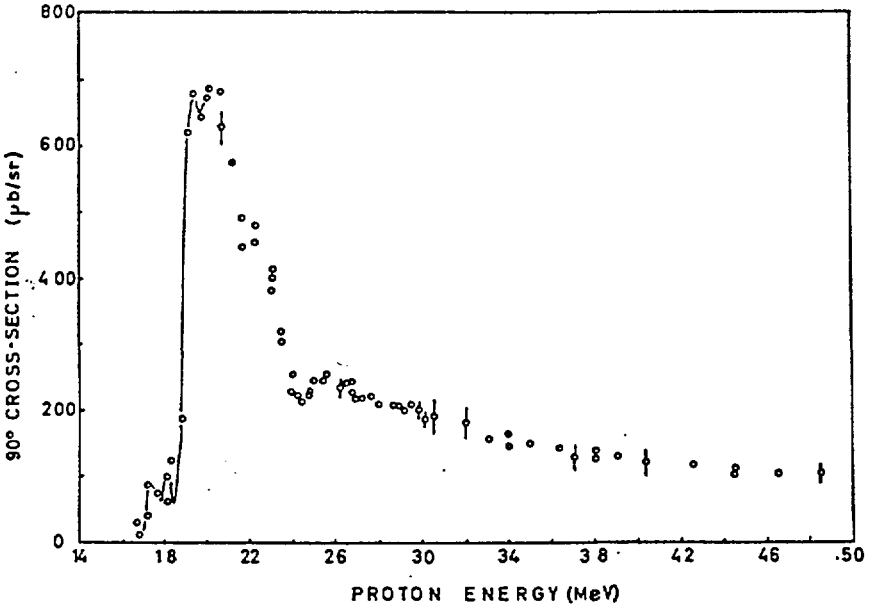

The excitation function for 15.1 MeV radiation following inelastic proton scattering. The solid line follows the results of Warburton and Funsten scaled down by a factor 0.80.

List of references

[Ala74] J.P. Alard, A. Baldin, J.P. Costilhes, J. Fargeix, R. Roche, J.C. Tamain, Nuovo Cimento (Letters) **19**(1974)841

[All64] R.G. Allas, S.S. Hanna, L. Meyer-Schutzmeister, R.E. Segel, Nucl. Phys. **58**(1964)122

[Alm59] E. Almqvist *et al.*, Phys. Rev. **114**(1959)1040

[Ang83] M. Anghinolfi, P. Corvisiero, G. Ricco, M. Taiuti, A. Zucchiatti, Nucl. Phys. **A399**(1983)66

[Ba55] G.A. Bartholomew, F. Brown, H.E. Gove, A.E. Litherland, E.B. Paul, Can. J. Phys. **33**(1955)441

[Bai55] J.K. Bair, J.D. Kington, H.B. Willard, Phys. Rev. **100**(1955)21

[Bar66] A.C.L. Barnard, J.B. Swint, T.B. Clegg, Nucl. Phys. **86**(1966)130

[Bec63] J.A. Becker, J.D. Fox, Nucl. Phys. **42**(1963)669

[Ber76] D. Berghofer, M.D. Hasinoff, R. Helmar, S.T. Lim, D.F. Measday, K. Ebisawa, Nucl. Phys. **A263**(1976)109

[Blu66] L.N. Blumberg, E.E. Gross, A. Van der Woude, A. Zucker, R.H. Bassel, Phys. Rev. **147**(1966)812

[Bra72] C. Brassard, H.D. Shay, J.P. Coffin, W. Scholz, D.A. Bromley, Phys. Rev. **C6**(1972)53

[But59] J.W. Butler, NRL Report 5282, Washington, D.C., (1959)

[Chi97] S. Chiba, O. Iwamoto, Y. Yamanouti, M. Sugimoto, M. Mizumoto, K. Hasegawa, E.S. Sukhovitskij, Y.V. Poradzinskij, Y. Watanabe, Nucl. Phys. **A624**(1997)305

[Cle61] A.B. Clegg, K.J. Foley, G.L. Salmon, R.E. Segel, Proc. Roy. Phys. Soc. **78**(1961)681

[Con57] H.E. Conzett, Phys. Rev. **105**(1957)1324

[Cor59] J.C. Corelli, E. Bleuler, D.J. Tendam, Phys. Rev. **116**(1959)1184

[Cr56] D.S. Craig, W.G. Cross, R.G. Jarvis, Phys. Rev. **103**(1956)1414

[Dae64] W.W. Daehnick, R. Sherr, Phys. Rev. **133**(1964)B934

[De57] J. De Veiga Simao, J.P.F. Sellschop, Phys. Rev. **106**(1957)98

[Del83] R. De Leo. G. D'Erasmo, A. Panteleo, M.N. Harekech, E. Cereda, S. Micheletti, M. Piganelli, Phys. Rev. **C28**(1983)1443

[Dic63] J.K. Dickens, D.A. Haner, C.J. Waddell, Phys. Rev. **132**(1963)2159

[Dic63a] J.K. Dickens, D.A. Haner, C.J. Waddell, Phys. Rev. **129**(1963)743

[Dye81] P. Dyer, D. Bodansky, A.G. Seamster, E.B. Norman, D.R. Maxson, Phys. Rev. **C23**(1981)1865

[Emm66] J.M. Emmerson, J.C.W. Madden, C.M.P. Johnson, N. Middlemus, A.B. Clegg, W.S.C. Williams, Nucl. Phys. **77**(1966)305

[Fan67] J.H. Fannon, E.J. Burge, D.H. Smith, N.K. Ganguly, Nucl. Phys. **A97**(1967)263

[Fir96] Tables of Isotopes, ed. R.B. Firestone, V.S. Shirley, Wiley & Sons Inc., N.Y., (1996)

[Gem59] D.S. Gemmell, A.H. Morton, E.W. Titterton, Nucl. Phys. **10**(1959)33

[Ger75] H.V. Geramb, K. Amos, R. Sprickmann, K.T. Knopfle, M. Rogge, D. Ingham, C. Mayer-Boricke, Phys. Rev. **C12**(1975)1697

[Gov61] H.E. Gove, A.E. Litherland, R. Batchelor, Nucl. Phys. **26**(1961)480

[Han60] S.S. Hanna, R.E. Segel, Proc. Roy. Phys. Soc. **A259**(1960)267

[Ho55] R.E. Holland, D.R. Inglis, R.E. Malm, F.P. Mooring, Phys. Rev. **99**(1955)92

[Hor70] Y.S. Horowitz, R.E. Bell, Can. J. Phys. **48**(1970)204

[Hos78] K. Hosomo, M. Kondo, T. Saito, N. Matsuoka, S. Nagemichi, S. Kato, K. Ogino, Y. Kadota, T. Noro, Phys. Rev. Lett. **41**(1978)621

[Hu53] T. Huus, R.B. Day, Phys. Rev. **91**(1953)599

[Kat80] S. Kato, K. Okada, M. Kondo, A. Shimizu, K. Hosono, T. Saito, N. Matsuoka, S. Nagamichi, K. Kisimura, N. Tamura, K. Imai, K. Egawa, M. Nakamura, T. Noro, H. Shimizu, K. Ogino, Y. Kado, Nucl. Instr. Meth. **169**(1980)589

[Ker69] G. Kernel, W.M. Mason, Nucl. Phys. **A123**(1969)205

[Led78] E. Brown, J.M. Dairiki, R. Doebler, A.A. Shahib-Eldin, L.J. Jardine, J.K. Tuli, A.B. Buyrn, Tables of Isotopes, ed. C.M. Lederer, V.S. Shirley, Wiley & Sons Inc., N.Y.,(1978)

[Mat75] J.L. Matthews, D.J.S. Findlay, S.N. Gardiner, R.O. Owens, Nucl. Phys. **A267**(1975)51
[Mea63] D.F. Measday, P.S. Fisher, A. Kalmykov, F.A. Nikolaev, A.B. Clegg, Nucl. Phys. **44**(1963)98
[Mea73] D.F. Measday, M.Hasinoff, D.L. Johnson, Can. J. Phys. **51**(1973)1227
[Mei85] A. Meigooni, R.W. Finlay, J.S. Petler, J.P. Delaroche, Nucl. Phys. **A445**(1985)304
[Mit64] G.E. Mitchell, E.B. Carter, R.H.Davis, Phys.Rev. **133**(1964)B1434
[Ols89] N. Olsson, B. Trostell, E. Ramstrom, Nucl. Phys. **A496**(1989)505
[Ram79] R. Ramaty, B. Kozlovsky, R.E. Lingenfelter, Astrophys. J. **S40**(1979)487
[Rei56] C.W. Reich, G.C. Phillips, J.L. Russell, Phys. Rev. **104**(1956)143
[Sco67] D.K. Scott, P.S. Fisher, N.S. Chant, Nucl. Phys. **A99**(1967)177
[Sat67] G.R. Satchler, Nucl. Phys. **A100**(1967)481,497
[Sno77] K.A. Snover, P. Paul, H.M.Kuan, Nucl. Phys. **A285**(1977)189
[Sno68] K.A. Snover, E.G. Adelberger, F.Riess, Bull. Am. Phys. Soc. **13**(1968)1662
[Sto64] T. Stovall, M. Hintz, Phys. Rev. **135**(1964)B330
[Suk98] E.S. Sukhovitskij, S. Chiba, O. Iwamoto, Y.V. Porodzinskij, Nucl. Phys. **A640**(1998)147
[Swi66] J.B. Swint, A.C.L. Barnard, T.B. Clegg, J.L. Weil, Nucl. Phys. **86**(1966)119
[Tyr57] H. Tyren, T.A.J. Maris, Nucl. Phys. **4**(1957)637
[War62] E.K. Warburton, H.O. Funsten, Phys. Rev. **128**(1962)1810
[Yav59] A.I. Yavin, G.W. Farwell, Nucl. Phys. **12**(1959)1
[Zob68] W. Zobel, F.C. Maienschein, J.H. Todd, G.T. Chapman, Nucl. Sci. Eng. **32**(1968)392

Nuclear Data Section
International Atomic Energy Agency
P.O. Box 100
A-1400 Vienna
Austria

e-mail: services@iaeand.iaea.or.at
fax: (43-1)26007
cable: INATOM VIENNA
telex: 1-12645 atom a
telephone: (43-1)2600-21710

online: TELNET or FTP: iaeand.iaea.or.at
username: IAEANDS for interactive Nuclear Data Information System
username: ANONYMOUS for FTP file transfer
username: FENDL for FTP file transfer of FENDL-1 files, FENDL2 for FENDL-2 files
For users with Web-browsers: http://www-nds.iaea.or.at